



BABEȘ-BOLYAI UNIVERSITY
Faculty of Environmental Science and
Engineering
Environmental Science Doctoral School



DOCTORAL THESIS

**IMPLICATIONS OF RADON RISK IN SMART BUILDING
DESIGN, CONSTRUCTION AND ARCHITECTURE**

SUMMARY

PhD Giagias Evangelos

Scientific supervisor:

Prof. Univ. Dr. DUMITRU RISTOIU

Coordinator:

Prof. Univ. Dr. CONSTANTIN COSMA

CLUJ-NAPOCA
2024

1	INTRODUCTION	3
2	PURPOSE OF THE RESEARCH	3
3	THESIS STRUCTURE	4
3.1	Chapter I.	4
3.2	Chapter II.	5
3.3	Chapter III.	6
	Methods of measuring radon, radon emanations from the soil, natural background radiation and radiation emitted by building materials.	6
3.3.1	Indoor radon	6
3.3.2	Activities of natural radionuclides in building materials.	8
3.4	Chapter IV.	9
3.5	Chapter V	13
3.6	Chapter VI	16
4	STUDY OF INDOOR RADON IN RESIDENTIAL DWELLINGS IN THE METROPOLITAN AREA OF ATHENS AND ARGOLIDA (PELOPONESE)	20
4.1	Geodynamic framework of the study area	22
4.2	Review of the geology and geotectonics of the ZMA and Argolida	26
4.3	Analysis methodology and statistical data processing	29
5	RADIOACTIVITY OF BUILDING MATERIALS FREQUENTLY USED IN GREECE	32
5.1	Measurement of radionuclide activity concentration	33
5.2	Radiological parameters for the studied materials	35
5.3	Conclusions.	37
6	SELECTIVE BIBLIOGRAPHY	37

Key words: Indoor radon, Radon risk, Natural radionuclides in building materials, climate change, smart buildings, Greece

1 INTRODUCTION

The objectives of the present study are;

a) Indoor Radon monitoring of 25 homes representative of the Athens Metropolitan Area (MAA) and Argolida region, Epidavros city (AR), using CR39 type trace detectors, exposed for three months in three seasons, Spring, Summer and Winter.

b) Analysis of the radioactivities of the primordial radionuclides U 238, Ra 226, Th 232 and K 40 from 18 samples of building materials frequently used in Greece and the estimation of the radon risk for humans,

c) Analysis of the radon risk due to its accumulation inside buildings, the contribution of radioactivity due to radionuclides present in construction materials,

d) The strategy that Architects and Builders must adopt in the face of increasing radon accumulations inside buildings due to their energy efficiency and thermal rehabilitation, taking into account the alteration of the climate by human factors.

2 PURPOSE OF THE RESEARCH

- ✓ determinarea și urmărirea variației concentrațiilor de radon de interior din 25 locuințe situate în Zona Metropolitană Atena și Regiunea Argolida, orașul Epidavros, pe parcursul a trei anotimpuri și a contribuției lor la doză,
- ✓ găsirea unei ipoteze plauzibile pentru valorile mari și foarte mari pentru locuințe situate în vecinătate în completarea celei emise la prima analiză a acestor rezultate (Giagias 2015).
- ✓ Cercetarea literaturii de specialitate cu privire la structura geologică a zonelor studiate și posibilelor legături cu emanațiile de radon,
- ✓ determinarea concentrațiilor de activitate ale K 40, Ra 226, Th 232 și U 238 din 18 probe de materiale de construcții utilizate frecvent în Grecia și contribuția lor la debitul dozei. Cunoașterea radioactivității prezente în materialele de construcție permite evaluarea oricărui pericol radiologic posibil pentru locuitorii unei case în funcție de diversitatea materialele folosite pentru construcția clădirilor. Rezultatele obținute pot servi drept date de bază pentru nivelul de radioactivitate în această arie studiată.

- ✓ Scoaterea în evidență a responsabilității arhitecților și constructorilor privind protecția locatarilor de acumulările de radon în spații închise fără aerisire adecvată,
- ✓ importanța cunoașterii; i). concentrațiilor de radon din case, ii) contribuția radiațiilor emise de materialele de construcții din care sunt făcute casele, iii) contribuția radiațiilor naturale γ la doza anuală totală și măsurile pe care trebuie să le întreprindă pentru a micșora efectele nocive ale acestor radiații anterior începerii proiectului/respectiv construcției oricărui imobil, indiferent de destinație, în conformitate cu reglementările naționale și internaționale.

3 THESIS STRUCTURE

The thesis is structured on 8 Chapters (including Conclusions and Bibliography). It also contains an Appendix and List of publications.

3.1 Chapter I.

It is dedicated to those who over a century ago laid the foundations of a new branch of physics, nuclear physics, Wilhelm Conrad Röntgen, Henri Becquerel, Marie Skłodowska-Curie, Pierre Curie, Ernest Rutherford, Frederick Soddy, etc.. Soddy, benefiting both by some exceptional mentors as well as by the knowledge accumulated in a relatively short period in this branch of physics, he predicted both the advantages of these discoveries such as;

- i) the development of modern radioactive dating techniques,
- ii) ii) that nuclear power could one day provide abundant, cheap and clean energy, ending pollution and poverty forever,
- iii) iii) also warned that its uncontrolled release could cause terrible destruction,
- iv) iv) his belief that nuclear war would be utterly disastrous for humanity has become part of the conventional wisdom of our time.

One of his last public acts was to join 17 other Nobel Prize winners in signing an appeal to world leaders to abandon nuclear weapons (Merricks 1996).

Also in Chapter I, there is a brief analysis of the properties of radon, the sources of radon in the soil and the earth's crust, the generation of radon in the soil and in rocks, respectively the presence of radon in different environmental factors: air, inside houses, water and underground.

3.2 Chapter II.

Brings up to date the responsibility of Architects and Builders in terms of the design and construction of new buildings that comply with national and international regulations regarding the maximum accepted limits for radiological risk factors generated by the accumulation of indoor radon in closed spaces, in the context of global warming, of climate change and the energy efficiency of buildings, for all new buildings but also of remedial solutions for already built buildings with indoor radon concentrations above the warning limit.

Climate change and the global warming of our planet has been one of the most debated topics in the earth, atmospheric and space sciences for the past 30 years. In 1975 Broecker launched the idea of global warming which was accepted by most scientists, (Broecker 1975). Some of them believe that climate change is mainly caused by human activity and increased emissions of greenhouse gases – especially CO₂. Others argue that Earth's climate depends on the influence of natural astronomical, physical, and geodynamic factors, including the sun's complex impact on climate, as well as the impact of Earth's orbital changes.

Astronomical and orbital factors are crucial to Earth's climate. Global climate change may be indirectly due to gravitational resonances generated by the large planets in the solar system and the Sun, or to the passage of the solar system through the five arms of the Milky Way Galaxy. These factors are also related to the brightness of the Sun; Earth's position in the solar system; the rotation of the Earth around its axis and around the Sun; rotation of the Solar System around the galactic center; the interaction between the Earth-Sun and Earth-Moon systems; the interaction with other bodies in the solar system and the peculiarities in the orbital motion of the Earth.

In principle, it advocates for a more in-depth study of the causes of global warming and the repercussions of this phenomenon in everyday life, emphasizing adaptation to climate change rather than the implementation of measures that are impossible to achieve in the terms proposed and insufficiently proven by the IPCC and their supporters with total disregard, or tacit acceptance, of the suggestions of tens of thousands of researchers who request it.

Certainly, the trend of global warming determined by natural factors is combined with the impact of greenhouse gases - especially CO₂ - and the role of man is crucial in this phenomenon. Of course, galactic cosmic rays also have an impact. That is why the Intergovernmental Panel on Climate Change (IPCC) when making various simulations of climate evolution for the near future must give more importance to natural factors. Temperature variations at the Earth's surface are much more numerous than the effects of greenhouse gases. Adherence to the roadmap set out in the Paris Agreement is unlikely to be met without serious human repercussions.

That's why *"both sides must be listened to!"* (Lutgens, 1992; IPCC, 2001).

The opinions of both sides are presented in detail, as well as the real problem that arises from the point of view of Radon. All the repercussions of the negative effects of global warming can be found in the additional exposure of the world's population to ionizing radiation, but especially in the increase in indoor radon levels as a result of

That is why it is absolutely necessary "Let the other side be heard" ("Audiatur et altera pars" Seneca, ca. 4 BC - 65 AD), valid so much in justice but also in science.

energy efficiency policies for all homes and public spaces up to "Zero-Energy Building (ZEB)" which implies major changes in the approach to this desired by Architects and Builders.

3.3 Chapter III.

Methods of measuring radon, radon emanations from the soil, natural background radiation and radiation emitted by building materials.

3.3.1 Indoor radon

It was considered that a description of all the methods and techniques for measuring Radon and the radioactivity of some radionuclides, present in construction materials, involved in affecting human health, would occupy too much space and would even be useless. Therefore, after briefly listing the history of the evolution of ionizing radiation detection methods and measurement techniques that have been perfected and are currently widely used, we proceed to describe the methods used in the present study.

The "raw" results and areas of provenance are presented for each method, reserving separate chapters for Analysis, Data Interpretation and Discussion on these topics. These are:

- the method for instantaneous radon measurements based on the scintillation cell. The first to develop and impose this technique was H.F. Lucas. The cell has deposited on the inner walls the scintillating material ZnS(Ag) (Lucas, 1957). An alpha particle produced by the decay of radon inside the cell strikes the scintillating material, generating a photon of light. This photon will be sensed and counted by a photomultiplier tube, which is optically coupled to the quartz window of the cell. The photomultiplier will convert the scintillation produced into an electrical pulse. The detection efficiency of the Lucas a cell is 75-80%, and it has a background of only 0.1 imp/min. Thus, the measurement error of a sample with a concentration of 10 Bq.m⁻³ in the sample and background with a pulse counter during three hours is about 30% (Lucas, 1957). Measurements on air samples are usually made after reaching the radioactive equilibrium between radon and its descendants (Po 218 and Po 214). The amount of radon in the cell is directly proportional to the number of decays observed above the background detection limit.

- the method based on solid-state nuclear trace detectors (SSNDs). This technique is widely used in indoor radon measurement studies (Cucos, et.al., 2012; Papp, et.al., 2012; Kinga 2015). Each detectable α -particle produces in a SSNTD a single damage track, which, after chemical development, transforms into a narrow channel that is visible under a microscope. For the most part, these SSNTDs are cellulose esters (nitrate and acetate) and polycarbonates such as bis-phenol-a polycarbonate and CR-39. An integrated system of the RadoSys 2000 type (manufacturer RadoSys, Budapest, Hungary) is used for reading the CR-39 trace detectors, consisting of the following components: RadoBath development unit, RadoMeter optical microscope and Laptop with appropriate software for reading traces and statistical processing

To measure radon gas concentrations in homes in Greece, a long-term assessment of domestic radon concentrations was undertaken using solid-state nuclear detectors (CR-39).

In this study, a number of 25 homes representative of the Athens Metropolitan Area and the Agolida region, Epidavros city, were monitored using CR39 track detectors, provided by the Hungarian company, RadoSys Ltd, exposed for three months in three seasons, Spring, Summer and Winter (Giagias et.al., 2015a, 2015b). At the end of the exposure period from the dwellings, the detectors were collected, properly packed in an envelope with an anti-radon filter, and transported safely for processing and analysis to the Center for Environmental Radioactivity and Nuclear Data at Babeş-Bolyai University, Cluj- Napoca, Romania. In the Laboratory, the detectors are extracted from the box (Radapot) in which they were exposed and inserted into the plastic supports (slides) specially built for development and the radon concentrations are determined by reading the traces left on the detector.

The locations where the detectors were installed and the results of primary data processing are also presented. In the Athens Metropolitan Area, 23 detectors were installed as follows: ATHENS SUD; 12 CR39 detectors (for the winter season 2 detectors were lost), PIRAEUS; 6 detectors, ATHENS NORTH; 2 detectors, ATHENS EAST; 3 detectors (for the winter period all three detectors were lost) and 2 detectors were installed in PELOPONEZ, ARGOLIDA region, EPIDAVROS locality.

3.3.2 Activities of natural radionuclides in building materials.

- The gamma spectrometry technique is used to measure the activities of radionuclides U 238, 232U, Ra 226 and K 40. According to the timeline of the basic safety standards of the European Union—EU BSS—(Council of the European Union 2014), all EU members should apply these requirements by 2018. Reducing the concentration of radon below the recommended level may be a new challenge for building materials. constructions used for homes, public spaces but also for work areas, such as underground mines or caves. One of the most accurate and widely used methods is Gamma Spectrometry (Cosma, et.al., 2012).

A high-resolution gamma-ray spectrometer equipped with an ORTEC GMX 40–76 HPGe semiconductor radiation detector with a relative efficiency of 40% was used to evaluate all gamma-emitting materials, both qualitatively and quantitatively by detecting the amplitude and the energy level of the gamma photons emitted from the

isotopes and thereby determining the specific activity concentration of radionuclides Th232, 228Ra, Ra 226 and K 40 in rock samples. For quality assurance (QA) purposes in the analytical protocol, it is recommended that a certified soil standard be used. For compliance, the 312-standard provided by the International Atomic Energy Agency (IAEA (2007)) with a known activity concentration for the studied radionuclides was used.

The detector was covered with a 20 cm thick lead shield and a nickel layer all around to reduce the natural background flux. Data were analyzed with Aptec MCA Multichannel Analyzer software. More details on the gamma ray measurement used in this study can be found in (IAEA, 2007), Adelikhah M et.al (2020), Shahrokhi A, et.al. (2020). The detector is regularly calibrated according to IAEA protocols. Related information on the calibration process is presented in a previous publication (Shahrokhi A, et.al. 2021).

18 samples were collected from 18 building material stores in Attica, Greece for radioactivity assessment (Giagias E., 2017). In Table 3.5, the locations where the samples were collected, the types of construction materials most commonly used for single-family houses are presented.

All sample activities were calculated using IAEA standards. Th 232 was determined from the 238 keV (212Pb), 338 keV (228Ac), and 911 keV (228Ac) peaks, U 238 from the 92 keV (234Th) and 63 keV (234Th) peaks, and K 40 from 1460 keV. The measurement time in all cases was greater than 48 hours, a requirement necessary to obtain a large enough number of data to obtain the maximum required uncertainty of $\pm 10\%$, within the two-sigma confidence interval. The relative method was used to calculate the activity by keeping the same geometry and matrix between the sample and the certified reference materials (IAEA-312, 327 and 385).

3.4 Chapter IV.

It is dedicated to the study of indoor radon in 23 residential homes in the Athens Metropolitan Area and 2 in Argolida.

When structuring this Chapter were taken into consideration;

- a) The level of knowledge, on a global level, regarding the danger posed by Radon to human health correlated with the level of awareness in this field at the National level,
- b) Increasing interest in more in-depth studies on the distribution of radon on the Earth's surface,
- c) Development of accredited and commercially available measurement devices and techniques,
- d) Modern equipment and techniques available at the Center for Environmental Radioactivity and Nuclear Data at Babeş-Bolyai University, Cluj-Napoca, Romania,
- e) Establishing international collaborations between this Center and Research Institutions and Groups, mainly from Europe,
- f) The results obtained by this Center and the interest to extend its studies also in Greece,
- g) The results obtained after developing the detectors, counting the traces on the detectors and converting them into average values of Radon concentrations, for the 75 detectors placed in 25 homes in Greece during three seasons, were also tabulated according to the site index where detectors and seasons were mounted.
- h) The results were published (Giagias 2015a, 2015b) and in conclusion it was established that there is a seasonal variation of radon concentrations and the large deviations from the average values were attributed to the lack of ventilation,
- i) Taking into account the knowledge gained internationally and the development of Radon Maps for most countries in Europe, we considered it necessary to revise our results relative to the values extracted from the Radon Map of Greece, which we took as a reference point ,
- j) It was concluded that the existing geology and seismotectonic activities in the area could explain these deviations from the values specified on the map,
- k) Studies older or subsequent to this study also mentioned extreme values of radon concentrations without attributing them directly to geology.

The first part of Chapter Four presents geographical, geological and geophysical data of the study area, Athens Metropolitan Area (MAA) and Argolis (Peloponnese) Greece, which could be useful in interpreting the final results. How both climatic and Geophysical factors affect, over time, the values of radon concentrations.

The effect of geophysical factors on human health and behavior is not imagination or fantasy. There is an increasing number of papers in recent years demonstrating the correlation between geomagnetic field (GMF) variations and human health parameters. Many theoretical hypotheses have been put forward in search of the plausible mechanism by which living systems and human beings perceive and react to changes in GMF.

The basic geophysical and environmental factors that could affect human health and behavior are: changes in solar activity, GMF variations, meteorological changes as well as changes in geochemical and tectonic processes. There are facts that all could influence each other. That is why it is very difficult to separate the various influences and it is very easy to miss the effects on human beings. It can be summarized that the whole human body, mental reactions and behavior respond to sudden changes of various types in GMF. Our attention for now is only focused on the influence of these factors on the most accurate prediction of radon emanations, their accumulation inside buildings, the risk they present to the health of people who work in such places and what measures must be taken to reduce these risks.

The study of indoor radon concentration variations both on the world map and in Greece is a concern of the greatest interest. To date there have been several small- and medium-scale studies Nikolopoulos et.al., (2013) and two other large-scale radon studies: one conducted over a long period of time (from 1995 to 1998) using trace detectors fitted in 1277 homes, carried out by the University of Athens and one from 1999-2006 carried out by the team from the Laboratory of Nuclear Technology, Aristotle University of Thessaloniki, Clouvas et.al., (2009). passive radon detectors (electrets) were used in 561 workplaces the standard radon mapping grid consisting of cells with a side of 10x10 km was used to develop the map.

Although this type of map only provides indicative information, they have proven very useful to architects as a first assessment of the radon risk for the land on which buildings are to be built.

In terms of Climate due to its large area, metropolitan Athens has a variety of climates. Most of the Athens metropolitan area has a warm summer Mediterranean climate, while some areas of the Athens Riviera, the Thriasio Plain and some areas to the west have a warm semi-arid climate. The minimum daily average during the Winter period is between 7.1 °C for January and 9.2 °C for March and 8.7 °C for December. The average annual minimum temperature is - 6.5 °C. However, the maximum annual temperature reaches 44.8 °C so that during a year the difference between the minimum and maximum temperature reaches 51.35 °C. All these peculiarities of the climate must be taken into account when analyzing the results.

From the point of view of geophysical factors, the situation of Attica is a special one. The complexity of the geology of the Athens Metropolitan Area (AMA) is determined by: (a) the coexistence in the area of sedimentary and rocky bedrock formations; (b) stratigraphic and lithological heterogeneity; (c) the existence of similar lithological types in different formations, e.g. limestone from almost all geological formations of the AMA (Athena Shale, Athens Sandstone-Marl and the entire Athens Limestone, the Upper Cretaceous limestone hills at the foot of Mount Egaleo); (d) strong tectonic deformation; and (e) significant alteration of local rocks by water movement.

The Athens Metropolitan Area extends over the Athens Basin, a narrow Neogene-Quaternary wedge-shaped basin on the Attica peninsula, bounded to the west, north and east by the Egaleo, Parnitha, Pentelikon and Hymettus Mountains respectively, while to the south-west opens to the gulf of Thessaloniki. The Athens Basin is formed along the contact of the Pelagonic (or Sub-Pelagonic) lithotectonic unit in the northwest, with the Attic-Cycladic Complex in the southeast (Fig. 4.3).

Through the middle of the Athens Metropolitan Area runs an active shear fault that practically cuts it in two and in the four corners there are four more subduction or slip faults. There is an active volcano and dozens of hot springs with temperatures up to 100 °C. More details on these aspects are given in Annex 2.

Since Greece has a Radon Map, first the areas of interest were delimited and the average Radon values were entered, according to the results obtained at the time of drawing up this Map, Figure 4.5. and the annual effective dose was calculated for these values, Table 4.4. We chose this option to have a benchmark against our results.

The conduct of the experiment consisted in exposing the CR-39 detectors for three periods of three months each, from March 2013 to March 2014. The detectors were placed at a distance of at least 0.5 m from the wall and to obtain more representative samples of air from the breathing zone, as far as possible from windows and doors.

The results obtained at all the locations where the detectors were installed are analyzed and discussed in detail depending on the location of the respective location on the map of the study area, the period of exposure, the comparison of the results obtained with those on the radon map of Greece and the issuance of hypotheses regarding possible mismatches .

The obtained results are in good correlation with the geophysics of the study area resulting in a significant deviation from the radon map with a proportional increase for all seasons. The lowest values correspond to Spring and the highest to Winter.

Of the 25 houses subjected to the study, 15 have the average, over three seasons, of Radon concentrations below the minimum reference value (100 Bq.m^{-3}) and 10 houses below the action level (200 Bq.m^{-3}). Therefore, all 25 houses meet the regulatory measures provided by European legislation, but also those provided by Greek and Romanian legislation (UNSCEAR 2000). The distribution factor $R^2 = 0.9445$, indicates a surprisingly good correlation between the individual values corresponding to each season. It also indicates that the radon sources that contribute to the variation in indoor radon concentrations are the same following seasonal variations. The average values for the Effective Annual Dose, expressed in mSv/year, were: 1.56 for Spring, 2.75 for Summer and 3.94 for Winter. In conclusion, all 25 houses meet the regulatory measures provided by European legislation but also those provided by Greek and Romanian legislation (ICRP 65, 1994, UNSCEAR 2000) for dose.

Another survey carried out by the Nicolopoulos Group in the Attica region obtained results similar to those in the present study. The range of variation of average radon concentrations, obtained in the present study, was between 23 and 247 Bq.m^{-3} , (table 4.30) and the range of variation of radon concentrations obtained by the Nicolopoulos group was between 3.7 and 261 Bq.m^{-3} , table 4.39.

3.5 Chapter V

It focuses on the study of the radioactivity of construction materials commonly used in Greece. It starts from the presentation of the radioactive decay series, highlighting the contribution of Radium 226 and Thorium 232 to the generation of

Radon. Fortunately, it is estimated that 99.8% of ingested Thorium is eliminated by the body. It continues with the presentation of the sources of radon that influence indoor radon, after which the studies performed on the 18 samples of construction materials are presented.

The origin of naturally occurring radioactive materials dates back to the creation of the universe, being responsible for both terrestrial and extraterrestrial radiation. Most of the naturally occurring radioactive materials result from the decay chain of K 40, Ra 226 and Th 232 and are found in varying proportions in all soils and rocks. In soil samples, the measure of natural radioactivity is usually given by the specific activity of representative radionuclides: Ra 226 Th 232, K 40 and U 238 (NCRP, 1993).

Although the parent element, U 238 does not present adverse effects on the environment, inhalation of its daughter nuclide Ra 226 is known to present a high degree of risk to human organs, especially the lungs, leading to lung cancer (Giagias, et.al. , 2017).

Natural radioactivity in building materials is responsible for the internal and external radiation exposure of human populations living in housing made of such building materials (Karahan, & Bayulken, 2000; Yalcin, 2012; UNSCEAR, 1982). The distribution of natural radionuclides is not uniform across the Earth's surface, therefore understanding their contribution to indoor radon concentrations is important to quantify the exposure of the human population to NORM, as most people spend 80-90% of their lives indoors (UNSCEAR 1988a, UNSCEAR 1988b, UNSCEAR 1993).

Previous studies have shown that the average global indoor effective dose due to gamma radiation from building materials is estimated to be about 0.4 mSvy-1 (UNSCEAR 1993). The presence of natural radionuclides in building materials in an amount exceeding the internationally acceptable limit has received global attention (UNSCEAR 1993, Khan, et.al., 2020; Kant et.al., 2006; Maxwell, et.al.). The activity of radionuclides depends on the geological and geographical setting as well as the geochemical characteristics of the materials (Faheen, et.al., 2008; UNSCEAR 1988a).

Many studies have investigated radiological elements in various soil, sediment and rock samples. However, there is little or no information on the radiological hazards

associated with deposits of Marble, Natural Stone (used in smaller quantities), Cement, Brick, Mortar and Sand (indispensable in most construction).

The radiation exposure of the population can be increased appreciably by the use of construction materials containing above-normal levels of natural radionuclides of terrestrial origin such as K 40, Ra 226, Th 232 and U 238. The important radiological consequences of natural radioactivity in building materials construction are twofold: (1) irradiation of the human body with gamma rays and (2) irradiation of lung tissues with ^{222}Rn , especially through its decay products.

The eighteen samples, consisting of different materials commonly used for the construction of buildings, were randomly collected from different localities on the territory of Greece, in accordance with the guide for the collection of samples from the environment for analysis (IAEA 1989). Each sample was given a unique identification index. During the collection of the samples, the coordinates of each sampling site were recorded using the GPS global positioning system with the Garmin eTrex 309 device. The collected samples were packed and transported safely to the Center for Nuclear Data and Environmental Radioactivity, Babeş-Bolyai University, Cluj -Napoca, Romania, for processing and analysis. Types of materials were as follows: Marble 8 samples, Natural stone 3 samples, Cement 3 samples Brick 2 samples, Mortar one sample and Sand one sample. The measurements were performed using a high resolution HPGe gamma spectrometric system (EG&GORTEC, GWL-120–15, USA) with 34.2% relative detection efficiency and determination time below 40,000 s ((Khan et.al. 2020)).

Equation 5.1 was used to calculate the activity concentrations of radionuclides Ra 226, Th 232 U 238 and K 40. Detailed calculations for each of the radionuclide's Ra 226, Th 232 U 238 and K 40 for each sample are given in Calculation Sheets 5.4 - 5.13 in Appendix 1.

Table 5.4 shows the concentrations of radionuclide activities, U 238, Th 232, Ra 226, and K 40 in (Bq/kg), determined from the gamma spectra for each sample. For the statistical processing of the data, from table 5.5, it was done with the Excel 2019 utility by replacing the detection limits with their numerical values. The main results obtained are:

- U 238, AM is 12.21 (Bq/kg); confidence interval = 5.69 (Bq/kg), for $\alpha = 0.05$;
Confidence interval value = 12.7 ± 5.69 (Bq/kg),
- ²³⁴Th, AM is 9.01 (Bq/kg); confidence interval = 5.08 (Bq/kg), for $\alpha = 0.05$;
Confidence interval value = 8.94 ± 5.08 (Bq/kg),
- Ra 226, AM is 26.89 (Bq/kg); confidence interval = 15.71 (Bq/kg), for $\alpha = 0.05$;
Confidence interval value = 26.88 ± 15.71 (Bq/kg),
- K 40, AM is 111.07 (Bq/kg); confidence interval = 111.07 (Bq/kg), for $\alpha = 0.05$;
Confidence interval value = 111.07 ± 68.22 (Bq/kg)

Special attention was paid to the calculation of the radiological hazard indices for each individual sample and then for each group of the studied materials.

The average activity concentration values were: 137 ± 39.9 (Bq/kg) for K 40, range 2.3 - 548.0 (Bq/kg); 31.6 ± 11.6 (Bq/kg) for Ra 226, range 0.7-184.5 (Bq/kg); 10.3 ± 3.1 (Bq/kg) for Th 232, range 1-48.3 (Bq/kg) and 11.4 ± 11.3 (Bq/kg) for U 238, range 1-74.2 (Bq/kg), the last line in table 5.6.

By comparing the average values of the typical activity concentration for materials from categories similar to those studied, presented in tables 5.7 and 5.8, namely 38.3 (Bq/kg) for Ra 226, 33.3 (Bq/kg) for Th 232 and 425 (Bq/kg) for K 40, Table 5.7, and 25 (Bq/kg) for Ra 226, 25 (Bq/kg) for Th 232 and 370 (Bq/kg) for K 40, Table 5.8. we find that all are lower or close to the average values table 5.5 and therefore meet the requirements of the regulations in force.

Analyzing the individual values of the activity concentrations for each sample and for each of the radionuclides K 40, Ra 226 and Th 232, we find that the average values of the activity concentrations do not correctly reflect the particularity of each sample, some exceeding the recommended values. For this reason, all calculations are repeated for each group of materials separately. The results for the 18 parameters studied for each individual sample are presented in table 5.9 and 5.9 continuation.

3.6 Chapter VI

It aims to highlight the multitude of requirements that Architects and Builders must implement in their projects to deal with global warming and energy efficiency, especially in homes, public spaces and workplaces.

It is likely that the health problems associated with the built environment began when cave dwellers struggled to evacuate smoke from their primitive shelters. Hippocrates, Greek philosopher and "father of medicine" was one of the first known individuals to rationally examine the nature of adverse health effects in work and living spaces. In his treatise, *On Air, Water, and Places*, Hippocrates hypothesized that disease was a direct manifestation of an "unhealthy place" rather than a form of punishment from angry gods. The quality of air, water, food, and general living conditions, along with the climatic elements of wind, sun, and rain, all contributed, according to Hippocrates, to the well-being of individuals (Samet & Spengler, 1991).

During the last two decades global warming and climate change are becoming major problems for human society. Buildings, both commercial and residential, contribute significantly to energy consumption (Lin, 2011). Energy consumption in buildings increases significantly annually due to increased human comfort needs and services (Shehadi, 2018). Apart from weather conditions, there are many factors that affect the energy consumption used for cooling and heating of buildings, such as wall structure, window-to-wall ratio and building orientation (Dong, 2010, Gellings, 2009). To exploit this potential and shape the fast-growing construction sector in a sustainable manner, appropriate funding schemes and policies as well as effective technologies need to be implemented urgently (UNEP 2021).

Due to increasing awareness of the vulnerability of the Earth's ecological environment, environmentalists have promoted passive energy conservation design since the end of the 20th century. Following the accelerated growth of the greenhouse effect and the global energy crisis, the beginning of the 21st century has forced the world to choose between sustainable passive design that saves energy and active energy-consuming design that satisfies the need for comfort. This has led to the new paradigm of intelligent energy use. Communities and their tenants should use new methods such as sensors, storage batteries and energy converters to improve the environmental conditions in homes (Capelli, 2006).

The key feature of an autonomous home is the use of green energy technology to reduce environmental load while creating a sustainable, high-quality and comfortable living environment. In the field of architecture, “autonomy” has two implications: autonomous control and self-sufficiency (Harper, 2009). Autonomy means that one can independently manage one's own consumption and make independent decisions without the influence or control of others (The American Heritage, 2009; Yourdisctionare, 2008). Self-sufficiency means that one can maintain self-sufficiency in resources such as food, water and energy (Moench, 2004) by contributing to the rational use of resources.

In architecture, simple, self-contained houses refer to the dwellings of nomadic peoples. Of course, nomadism is also seen as an exemplary self-sufficient lifestyle. In the field of environmental protection, autonomy has recently become a key principle in green energy technologies and water resource management (Lampinen, 2004; Voss, 1996).

The revised Energy Performance of Buildings Directive (2010/31/EU, 2018/844/EU) provides for an EU energy efficiency target of 32.5% for 2030 with an upward review clause until 2032. International Energy Agency (IEA, 2014, IEA 2021) also noted that while there is potential for significant health and well-being benefits associated with improved energy efficiency; it is also documented that, if energy efficiency measures are implemented incorrectly, they can have a negative impact on indoor environmental quality (IEQ) and therefore on health and well-being.

New building concepts often apply new and innovative technologies in construction, heating and ventilation. The effect of these technologies on other important aspects, such as indoor air quality, must be analyzed.

One of the important substances that contaminates indoor air is radon, a radioactive noble gas. Building-specific factors such as cracks, crevices, holes, etc. in building foundations, pressure differences across the building envelope (stack effect) that act as driving forces for convective entry of soil radon, and ventilation rates control indoor radon levels (in association with soil radon concentration and soil permeability from under the building).

Changing the energy characteristics of a home that reduce heat loss can affect the tightness of the building and implicitly the quality of the air inside. By reducing the flow of natural ventilation, there is an accumulation of pollutants that reach the interior of the building, including radon. (Korniyenko, 2018; Nero, 1983). The increase of radon concentration inside the building after rehabilitation to reduce heating loss has been studied in different countries. Several-fold increase in radon concentration was evidenced in certain single-family houses after the installation of new PVC windows in regions with high geogenic radon potential in the Czech Republic (Milner, 2014). In France, technical measures were taken to reduce heat loss from buildings by more than half, which resulted in the geometric mean radon concentration increasing by 1,615. Also, increased radon concentration has been observed in modernized houses in Switzerland (Burkart, 1984; Pampuri, 2018) and Germany (Meyer, 2019). In England, measures to reduce the permeability of the envelope of single-family houses resulted in a decrease in uncontrolled ventilation by an average of 1.9 times (Milner, 2014) and an increase in radon concentration by about 1.7 times (Symond, 2019).

The adverse health effects of radon are well documented (eg WHO, 2009). Therefore, regulation and mitigation are being considered which, among other measures, require knowledge of the geographic extent of the radon hazard. Radon risk is often defined as the probability that indoor radon will exceed a risk; the geogenic source of hazard (or potential risk) at a location or over an area is well described by its geogenic radon potential (GRP). Knowing the GRP of an area can support the decision whether additional local measurements are required in areas of planned development. Factors influencing indoor radon concentration are living habits such as ventilation and building structure, including building material or the presence and type of basement and cellar under the house.

The geogenic radon potential (GRP) describes the indoor radon source potential "that the Earth provides" because, in general, the subsoil (radon concentration in soil gas) is the main source for indoor radon concentration (UNSCEAR, 2000) . GRP is independent of the influence of any factors related to the building or living habits. In addition, the relationship between soil gas radon concentration and indoor radon

concentration is well known (Appleton & Miles, 2010; Chen et.al., 2010; Kemski et.al., 2005).

The Joint Research Center of the European Commission is focusing on the preparation of maps of the Geogenic Radon Potential (GRP), which differ substantially from the classical radon maps, would allow a better prediction and estimate the radon risk with sufficient precision in any area from the map using as input data already existing databases such as climatic, geological, natural radiation, seismic and tectonic in order to quantify the GRI on more compact areas where buildings should be built or recreational spaces arranged through a matrix with cells under 500 m, depending on the evaluated surface.

4 STUDY OF INDOOR RADON IN RESIDENTIAL DWELLINGS IN THE METROPOLITAN AREA OF ATHENS AND ARGOLIDA (PELOPONESE)

Au fost selectate cinci zone de studiu (Atena Sud, Atena Nord, Atena Est, Piraeus - cunoscută ca Zona Metropolitană Atena sau Atena Mare (great Atena) la acestea se adaugă și zona Argolida, orașul Epidavros din regiunea Peloponez, toate ținând de Provincia Attica.

Attica, care cuprinde întreaga zonă metropolitană a Atenei, capitala țării și cel mai mare oraș, este o regiune foarte aglomerată, care se întinde pe aproximativ 3808 km² are puține parcuri și zone verzi. Populația permanentă a crescut la 3,8 milioane de locuitori în 2011, cu o densitate de 1250 de locuitori/km², din care peste 95% sunt locuitori ai zonei metropolitane Atenei (Hellenic Statistics Authority; <https://www.statistics.gr/statistics/pop>).

The *region of Attica* is a triangular peninsula that stretches into the Aegean Sea and is watered by the bays of the Aegean Sea. In the center of the peninsula, there is a large basin in which the entire Athens-Piraeus metroplex (contiguous metropolitan area) was built. This basin is surrounded by four mountains: Hymettus, Parnitha (the highest mountain in Attica), Egaleo and Penteli (Figure 4.1), providing significant amounts of vegetation.

According to the Hellenic National Meteorological Service (HNMS), Attica is one of the warmest regions in Greece, with mean monthly temperatures and precipitation ranging from 8.8 °C to 28.3 °C and from 1.6 mm to 12.5 mm (HNMS 2023). Regarding the entire Attica peninsula, the lowest average annual rainfall is found in Anavysos, the Athenian Riviera with about 310 mm, while the highest average annual rainfall is found in Ippokrateios Politeia with

over 870 mm. Investigating the synergies between urban heat islands and heat waves in Athens, (Founda & Santamouris 2017) found positive feedback between the factors, which can lead to increased thermal risk in cities.



Fig. 4.1. Geographical position and topographical context of the Attica region (the black line and red arrow in the figure represents the outline of the space subtended by . Attica) (accessed 1 February 2023).

Local meteorological phenomena, such as changes in precipitation rates, lightning frequency, and cloud and fog formation, can be strongly affected by urban heat islands (Orville, et.al., 2001; Shem, & Shepherd, 2009). Instead, one of the key factors influencing the development and intensity of an urban heat island is local weather conditions. In this context, numerous studies have been undertaken to find the influences of single climate variables (wind speed, cloud cover, relative humidity and precipitation) on the size of the urban heat island (Ngarambe, et.al., 2021; Giannaros, & Melas, 2012 ; Wang, et.al., 2015; Santamouris, et.al., 2017).

The Athens metropolitan area covers 2,929 km² in the Attica region and includes a total of 58 municipalities, which are organized into seven regional units, Table 4.1. According to the 2021 census it reached a population. of 3,744,059. The municipalities of Athens and Piraeus serve as the two metropolitan centers of the Athens Metropolitan Area. There are also some inter-municipal centers that serve specific areas. The Urban Area of Athens, also known as Greater Athens (Greece).

Due to its large area, metropolitan Athens has a variety of climates. Most of the Athens metropolitan area has a hot summer Mediterranean climate, while some areas of the Athens Riviera, some areas of the Thriasio Plain, and some areas to the west have a warm semi-arid climate. According to the weather stations of the National Observatory of Athens and the Hellenic National Meteorological Service, the northern areas have wetter and colder winters while the southern areas have very mild winters.

Piraeus has a warm semi-arid climate and, according to the climate atlas of the Hellenic National Meteorological Service, is the only area in Attica, Greece that clearly falls into this climate category. Due to the Athens summer night land breezes, Piraeus experiences high summer minimum temperatures, while the average annual temperature is 19.4 °C.

The Peloponnese is a peninsula located at the southern tip of the continent, with an area of 21,549.6 km² and constitutes the southernmost part of mainland Greece. It is connected to the mainland by the Isthmus of Corinth. The peninsula has a mountainous interior and deeply indented coastlines.

The Argolis regional unit is subdivided into 4 municipalities. These are: Argos-Mykines, Epidaurus (Epidavros), Ermionida, Nafplio. The region of Epidaurus, a place with a rich history, belongs to the prefecture of Argolis in the northeastern part of the Peloponnese. It owes its name to the ancient theater of Epidaurus, the best-preserved ancient theater in Greece, which is 15 km from the village. The weather for March is average; temperature around 15°C and at night it feels like 6°C. In March, Palaia Epidavros receives an average of 49.03 mm of rain and about 5 rainy days per month. The humidity is close to 72%.

4.1 Geodynamic framework of the study area

The complexity of the geology of the Athens Metropolitan Area (AMA) is determined by: (a) the coexistence in the area of sedimentary and rocky bedrock formations; (b) stratigraphic and lithological heterogeneity; (c) the existence of similar lithological types in different formations, e.g. limestone from almost all geological formations of the AMA (Athena Shale, Athens Sandstone-Marl and the entire Athens Limestone, the Upper Cretaceous limestone hills at the foot of Mount Egaleo); (d) strong tectonic deformation; and (e) significant alteration of local rocks by water movement.

The Athens Metropolitan Area extends over the Athens Basin, a narrow Neogene-Quaternary wedge-shaped basin on the Attica peninsula, bounded to the west, north and east by the Egaleo, Parnitha, Pentelikon and Hymettus Mountains respectively, while to the south-

west opens to the Saronic gulf. The Athens Basin is formed along the contact of the Pelagonic (or Sub-Pelagonic) lithotectonic unit in the northwest, with the Attic-Cycladic Complex in the southeast (Fig. 4.3). Pelagonia is the remains of a microcontinent, consisting of Paleozoic basement with Paleozoic-Mesozoic (mostly Triassic) carbonate cover. On top of this carbonate platform, Triassic-Jurassic West Vardar ophiolites were obscured during the Upper Jurassic to Lower Cretaceous (Doutsos et al. 1993). During the Upper Cretaceous, transgressive carbonates were deposited (Upper Cretaceous limestone in Fig. 4.3); sedimentation continued locally during the Paleocene-Eocene, with the deposition of flysch (for the Pelagonian stratigraphy Auboin., (1959); Clement and Guernet, 1971; Bonneau, 1984; Jacobshagen, 1986; Doutsos et al., 1993; Coleman et al.), 2020). The basement of the Athens Basin consists mainly of the Athens Platform (Papanikolaou et al., 2004) (Fig. 4.3), a local platform of Pelagonian origin that is found only in this area.

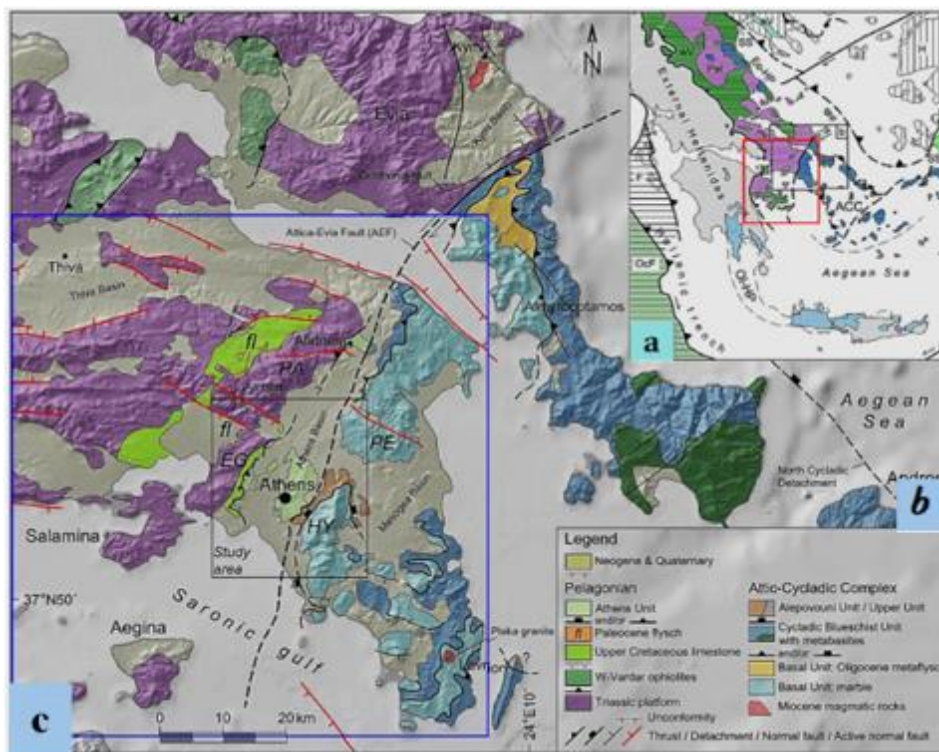


Fig. 4.3: Cadrul geologic al peninsulei Attica și sudul Eviei (Euboea). a) Privire de ansamblu simplificată și principalele caracteristici tectonice ale elenidelor (Schmid et al., 2020 cu modificări).și delimitarea zonei de studiu, (chenar roșu). b) Harta geologică și tectonică simplificată a zonei mai extinse a peninsulei Attica. PA: Muntele Parnitha, PE: Muntele Pentelikon, EG: Muntele Egaleo. (sursa: harta geologică a Greciei a HSGME; Xypolias et al., 2003; Spanos, 2012; Ring et al., 2007a; Deligiannakis et al., 2018; Tsoudoulos et al., 2007; Coleman et al., 2020; Boronkay, et al., 2021cu modificări). c) Detalii privind aria de studiu pentru Zona Metropolitană Atena, (chenar albastru).Adaptat după GeoMapApp (www.geomapapp.org)

This platform dates to the Upper Cretaceous (Turonian-Maastrichtian), several hundreds of meters thick, lithologically heterogeneous, metaclastic sequence with intercalations and alternations of carbonates and locally basic and ultrabasic igneous rocks (Marinos et al., 1971 and 1974).

The information about the Geology and tectonics of the Attica Region will allow a better interpretation of the results of the Radon measurements in this Region

Since Greece has a Radon Map, first the areas of interest were delimited and the average Radon values were entered, according to the results obtained at the time of drawing up this Map, Figure 4.5. and the annual effective dose was calculated for these values table 4.4. We chose this option to have a benchmark against our results.

The indoor ^{222}Rn study was carried out in 25 homes located in different sectors of the Athens Metropolitan Area (MAA) and is Argolida Sector, Peloponnese, shown in figure 4.6.

The elaboration of the Radon Map, figure 4.5, was done by administrative units, respectively Sectors, in the case of Athens. Average values of radon concentrations are calculated on the surface covered by a sector. The area of the Athens Metropolitan Area is 2929 km². A Sector has an area of approx. 300 km². The number of homes where radon monitoring was done is not evenly distributed over the surface of each sector for various reasons, so each Sector has a different number of locations.

Not having a standard for radon concentrations, it was considered normal to refer to the values listed on the radon map of each sector, table 4.4 where the value of the effective annual dose was also listed as the main risk factor for the health of the occupants of the residence.

Attica has always been one of the regions of Greece most exposed to natural hazards, especially earthquakes, floods, heat waves and forest fires. The high exposure of Attica and the Athens Basin in particular is due to the high concentration of population, activities, infrastructure and high-value stocks in a small area that is designated as a high natural hazard risk area. Figure 4.6 shows the ZMA map with the five sectors. The detectors were mounted as follows; 12 South Athens; 6 Piraeus; 2 Athens North and 3 Athens East.



Fig. 4.5 – Harta cu zonele de prelevare a Radonului de interior cu detectori de urme CR39 (adaptată după: <https://eeae.gr/en/radon-map>), unde: AN, înseamnă Atena Nord; AE, înseamnă Atena Est; AS, înseamnă Atena Sud; P, înseamnă Piraeus și AR, Argolida.

Tabela 4.4. The average values of the radon concentrations and the annual effective dose are presented in the adjacent table.

Radon map Greece	Average (Bq.m-3)	AED (mSv/an)
AS	29,00	0,83
PIR	47,00	1,35
AN	58,00	1,66
AE	62,00	1,78
AR	42,00	1,2

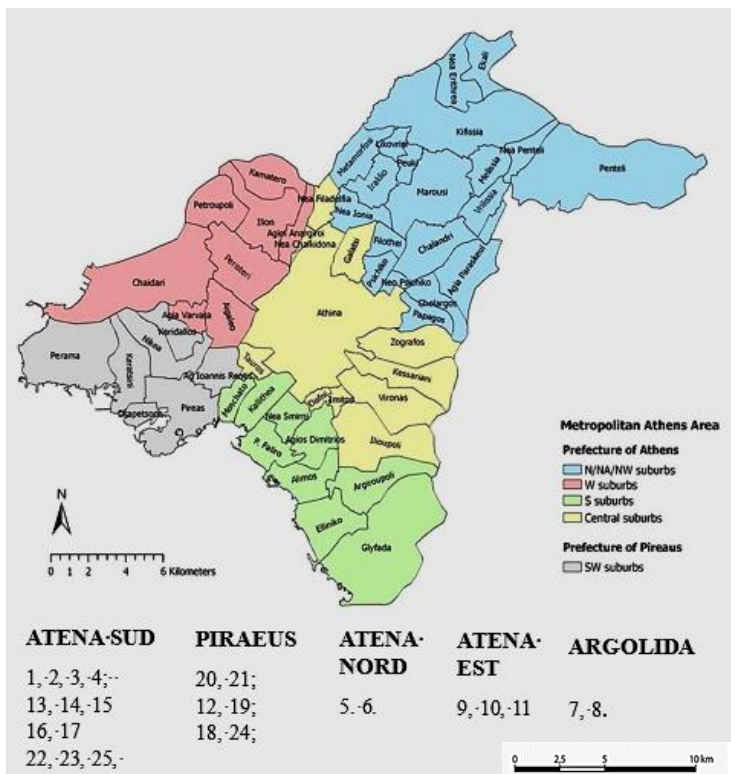


Fig.4.6 Compiled map; a) Athens Metropolitan Area; b) Indexes of Detectors by Sectors; and c) Argolida - Peloponnese sector.

The results obtained after the three monitoring seasons of the 25 homes were the subject of the article, "SEASONAL VARIATION OF INDOOR RADON IN DWELLINGS FROM ATHENS, GREECE" published in the magazine "Rom. Journ. Phys. 2015" Authors; E. Giagias, D. Burghel and C. Cosma. The map with the sampling points of this radon survey is the one in figure 4.6.1 1). And it is similar to the map in Figure 4.6 except that it does not refer

to the Digital Radon Map of Greece as it had not yet been completed. The obtained results show the existence of large fluctuations in the radon concentrations in the three series of measurements and we believe that "The differences between the values of the indoor radon concentrations R_n can be attributed to a wide range of factors, such as the geological setting, climatic parameters, building characteristics (e.g. level, type of building, presence of a basement, date of construction, type of ventilation, inhabitants)". The obtained results also highlight a seasonal variation of indoor radon concentration.

It was considered necessary to approach these variations from another point of view, especially since the authors did not exclude the influence of "a wide range of factors...". The natural question was asked. What other factors could "quasi-permanently" fuel indoor radon concentrations?

4.2 Review of the geology and geotectonics of the ZMA and Argolida

Referring to the Natural and Seismotectonic Hazard Maps it was found that the ZMA is furrowed by numerous faults and different geological structures, figures 4.6.1.2), 4.6.1.3) and 4.6.1.4) (Foumelis 2013).

The subsoil of Athens belongs to the alpine formations that outcrop in the mountains and hills of the area. Recent post-Alpine sediments (syn-rift deposits) often cover mountainsides as well as low-elevation areas. The area shows a complex alpine structure comprising mainly Mesozoic metamorphic rocks occurring at the Pendeli and Hymmetus mountains and Mesozoic non-metamorphic rocks of the Eastern Greek Geotectonic Unit occurring at the Parnitha, Poikilo and Aegaleo mountains, figure 4.6.1.4 (Foumelis 2013).

The boundary between the metamorphic and non-metamorphic geotectonic units, although it is generally accepted to be of tectonic origin, its exact geometric and kinematic characteristics have not yet been determined, as a direct geological mapping could not be carried out because it is covered by Neogene and Quaternary deposits, figures 4.6.1.2 and 4.6.1.3, (Papadopoulos et al. 2007).

The locality of Epidavros is also near a fault-lined area with numerous high-temperature hot springs and not far from an active Methana volcano, figure 4.6.1.5) (Tzanis et.al., 2020). Authors have shown that large-scale Quaternary plutonic magmatism in the NE Peloponnese is controlled by regional tectonics and occurs along the volcanic arc, along the axes of major extensional tectonic structures (Argolic Gulf and Plain, Hydra Strait) and along

the E-W transcurrent at local scale. faults that stretch across the Argolis Peninsula. The same principles and conditions appear to apply at local scales and shallower depths: the initiation and evolution of the MV and geothermal resources appear to be guided by the same tectonic activity that controls the plutonic magmatism of the wider area.

Analyzing the natural risk maps, it was hypothesized that it is possible that abnormal variations in the average values of radon concentrations in the studied areas if the homes where the detectors were installed are located near active faults, areas with high seismicity, even if the intensity of earthquakes is around 3 - 3.5 degrees on the Richter scale, of areas rich in hot thermal springs (temperature above 80 oC) or of active volcanic areas (Methane, for example).

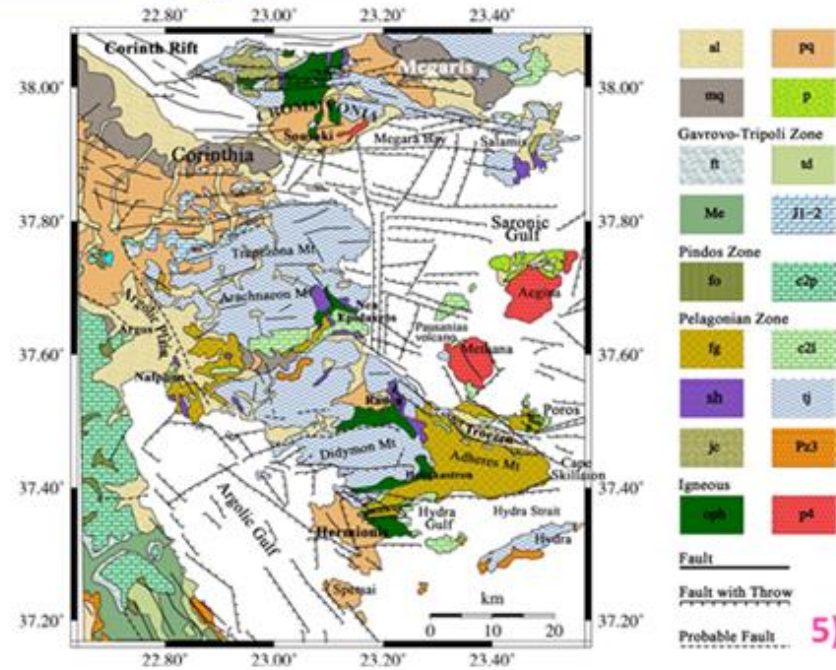
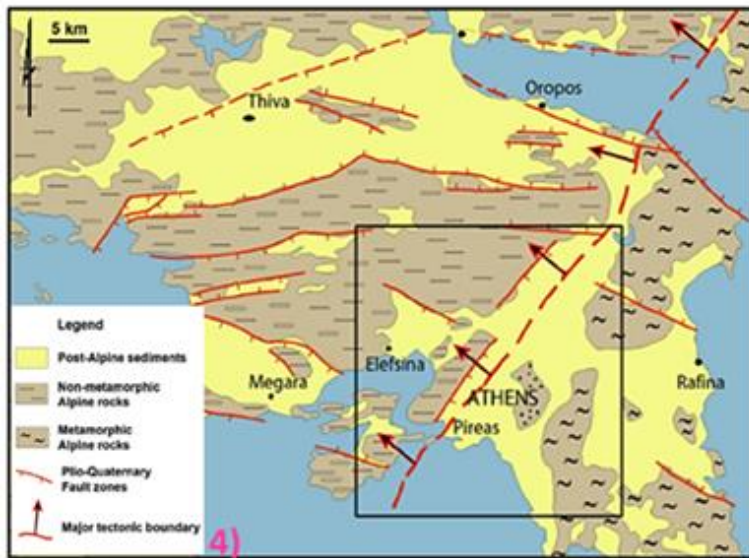
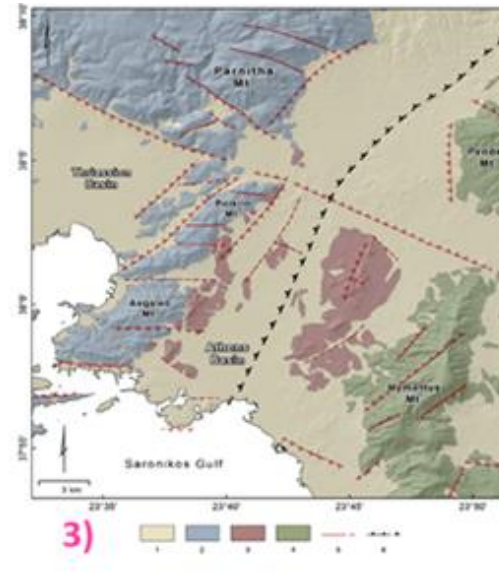
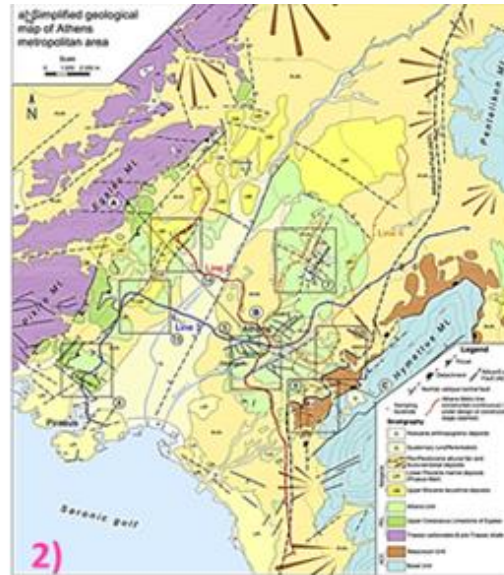


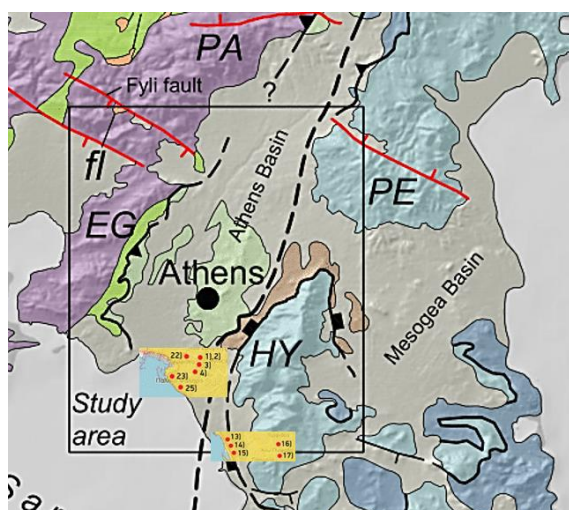
Fig. 4.6.1. Natural hazard maps that may influence radon emissions.

4.3 Analysis methodology and statistical data processing

The starting point is the map in figure 4.3. Figure 4.6.2 (2). It shows a cutout of a portion of this map where the average values of radon concentrations for the 4 sectors of the ZMZ according to the digital radon maps of Greece were pasted.. Another portion of the radon map of Greece was used for the Argolida sector , figure 4.6.2.(1).

The maps shown in figures 4.6.2 3a; 4a; 5a; 6 and 7 these zones were transposed on the radon map of Greece by sectors. Next, the sampling points were grouped into clusters, and the values measured with CR39 detectors represented graphically, in the form of PIE histograms. Cluster formation was based on the neighborhood criterion, to capture any local variation in radon concentrations, Figures 4.6.2. 3b; 4b and 5b.

In order to highlight possible anomalies, the statistical processing of the results is done both for all detectors (corresponding to the Piraeus sector) and by eliminating extreme values. The position of the house in relation to one of the high natural risk areas is then analyzed. If there is such a correlation, it means that the area presents a high risk of geogenic radon that contributes to the increase of indoor radon concentrations in the respective home. In the situation when the cluster contains only 2 locations, the situation is simplified and the result is easy to recognize.



A special situation can be found in the South Athens sector, figure 4.6.2.(4a), where the sampling points are very close to each other, and the clustering requires a more careful analysis of the natural hazard maps. All three maps in figures 4.2.6.1 2), 3) and 4) as well as figure 4.6.2. (2) indicates the presence of a major shear fault that "cuts" Athens in two but also the South Athens sector. This fault is most likely to pass between cluster group 1 and 2 and cluster group 3 and 4, figure 6.6.2.(4b). That is why it was decided that the statistical analysis of the data should be done both for all 12 detectors and separately for clusters.

Fig. f.n. The locations of the CR39 detectors in the Athens South sector, translated to scale, on a cutout in figure 4.3.

From figure f.n. it is very easy to see that all the locations in the South Athens sector are in the immediate vicinity of the faults that cross this area, which allows us to support the hypothesis that the anomalies in this area are due to geogenic radon. The detector locations for both the Athens East sector, Figures 4.2.6.(5a) and (5b), and the Athens North sector, Figure 4.2.6.(6), are also in the vicinity of the PE and PA faults.

For the Argolida sector the situation is even more obvious as the area is intersected by several active faults, thermal springs and is not far from an active volcano which is supposed to be the basis of these thermal springs.

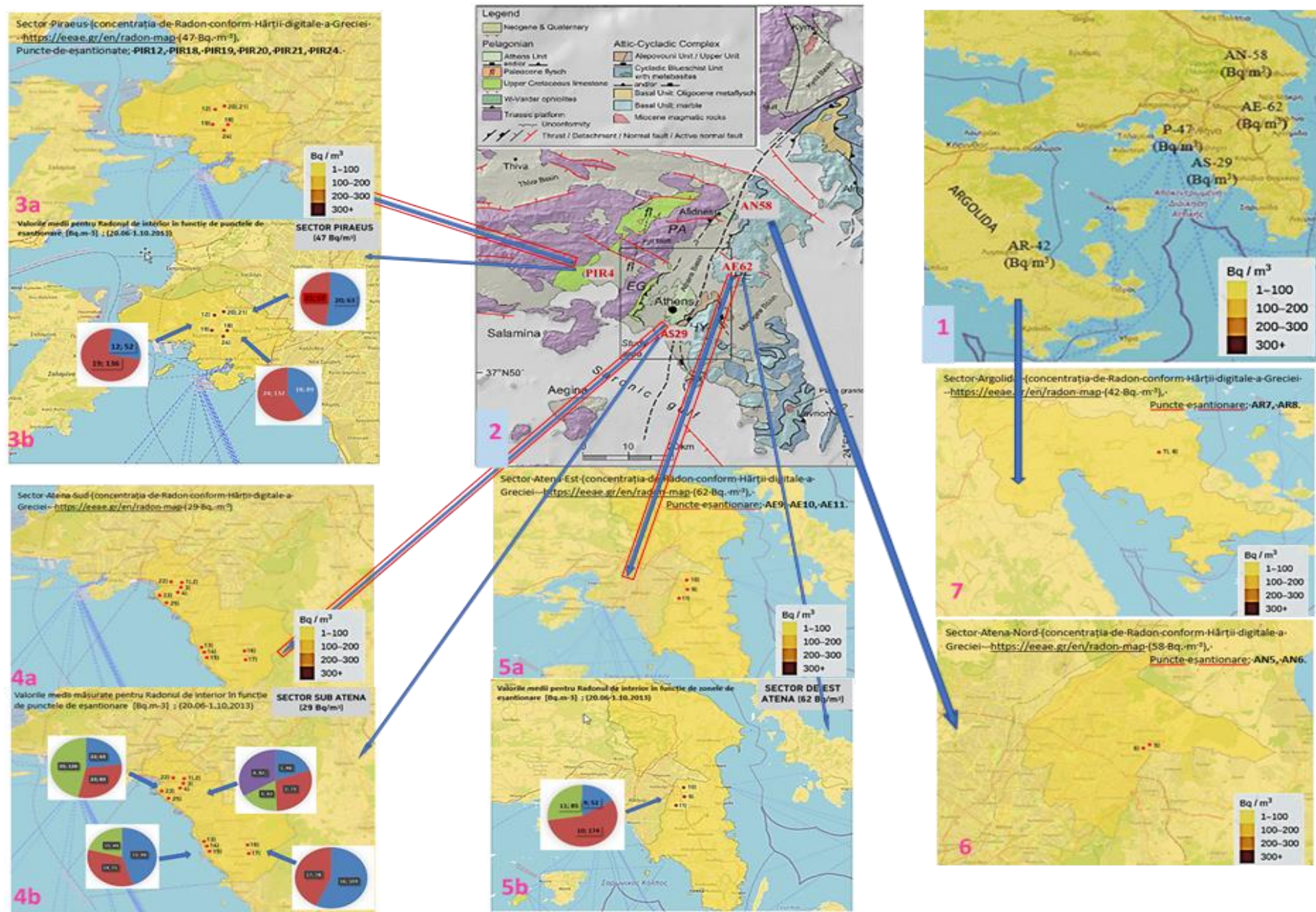


Fig. 4.6.2. Analysis strategy of the measurement results for the 25 detectors .

Table 4.5 shows the following information; Location indices, GPS coordinates of CR39 detector locations, exposure periods and unique indices of each detector, Radon concentration values, and Radon concentration values in (Bq.m-3) by Seasons and lastly the average value (AM) in every season. Unfortunately for the Winter period only 20 detectors could be recovered, 5 were declared Lost. This made data interpretation more difficult.

Table 4.5. Unique indexes to identify detector locations, GPS coordinates, indexes corresponding to each detector and radon concentration values..

Index LOC.	Primăvară 20/03/2013- 20/06/2013	Concentratia de Radon [Bq/m3]	Vara 20/06/2013- 20/09/2013	Concentratia de Radon [Bq/m3]	Iarna 20/01/2014- 20/3/2014	Concentratia de Radon [Bq/m3]
AS1	V78626	137	V79112	49	V78602	143
AS2	V78611	25	V78655	73	V79074	97
AS3	V79164	30	V79157	42	V79042	106
AS4	V79160	80	V79077	82	V78164	80
AN5	V79064	50	V78606	186	V79165	164
AN6	V79178	36	V78612	158	V78670	91
AR7	V78653	76	V79030	165	V79152	159
AR8	V79013	189	V78677	138	V79194	195
AE9	V79177	36	V79179	52	V78630	Pierduti
AE10	V79182	43	V79127	174	V75010	Pierduti
AE11	V79070	48	V78639	85	V75010	Pierduti
PIR12	V79019	85	V78603	52	V79155	246
AS13	V79080	33	V79186	94	V79170	111
AS14	V79169	81	V79053	71	V79106	175
AS15	V79192	23	V79148	44	V79101	133
AS16	V78623	35	V79025	103	V79190	165
AS17	V79075	52	V79093	78	V78675	140
PIR18	V79014	56	V79089	89	V79180	128
PIR19	V78662	44	V79196	136	V79035	155
PIR20	V79129	38	V79100	63	V79172	118
PIR21	V79113	25	V79195	63	V79159	89
AS22	V78601	37	V79061	63		Pierduti
AS23	V79119	31	V79015	83		Pierduti
PIR24	V78668	23	V78608	132	V79109	175
AS25	V79134	47	V79103	126	V79125	80
AVERAGE		54		96		137,00

The figures on Map 4.5 represent the average values of radon concentrations, in Bq.m-3, extracted from the radon map of Greece, corresponding to the homes where CR39 Radon detectors were installed. In each sector, several detectors were placed in different geographical and geological locations. The points where the CR39 radon detectors were placed as well as the average values of the radon concentrations and the annual effective dose are included on the map in figure 4.5 and table 4.4. These average values of radon concentrations from the Radon Map of Greece will be used as reference values and will be the basis for the intercomparison of the measurement results obtained with the CR39 detectors, during the three seasons; Spring - 20.03 – 25.06.2013, Summer - 20.06 – 01.10. and Winter 20.01 – 20.03. 2014.

The statistical analysis of the recorded levels of indoor radon concentrations and the distribution of the average radon concentration we used the Excel utility.

Each map shows the sector, the places and where the CR39 detectors were placed (the value estimated by the Digital Radon Map of Greece <http://eeae.gr/en/radon-map>, in the upper right corner, and in the PIE maps with the individual measured values of the radon concentrations determined following the development and reading of the solid CR39 nuclear trace detectors corresponding to each point.

The results will be presented by Sectors in the order of the seasons (for example; Athens South Spring, Athens South Summer, Athens South Winter, etc. for the following Sectors; Athens South (AS), Piraeus (PIR), Athens North (AN), Athens East (AE) and Argolis (AR) (located in the Peloponnese area).

5 RADIOACTIVITY OF BUILDING MATERIALS FREQUENTLY USED IN GREECE

Building materials can induce significant gamma radiation doses in closed spaces due to their natural content of radionuclides. Furthermore, they can also be a source of indoor radon. In recent years, a large database has been created with measurements of activity concentrations of natural radionuclides (Ra 226, Th 232, U 238 and K 40) from building materials (Khan, et.al. 2020). Knowledge of basic radiological parameters, such as the radioactive content of building materials, is important in assessing the possible radiation exposure of the population (Maxvell, et.al., 2018). It has been shown in various studies that if building materials with high concentration of natural radioactivity are used, indoor dose rates will increase accordingly (Ali, et.al., 1996). Naturally occurring radioactive material in rocks and soil contributes about 28 millirem or 8% of the radiation dose a person typically receives in a year from all sources, including medical exposures. Since radiation of natural origin is responsible for most of the total radiation exposure, knowing the dose received from these sources is very important not only for its effects on health, but also for the incidence of other radiation from artificial sources. (Fahnen, et al., 2008).

This study aims to determine the concentrations of natural radionuclides (Ra 226, Th 232 U 238 and K 40) and to assess its radiological risks in samples of natural raw materials frequently used for both domestic and industrial purposes in Greece.

Eighteen samples, consisting of different materials commonly used for the construction of buildings, were randomly collected from different localities in the territory of Greece, in accordance with the guideline for the collection of samples from the environment for analysis.

5.1 Measurement of radionuclide activity concentration

The activity concentrations of natural radionuclides (Ra 226, Th 232 U 238 and K 40) were determined and to evaluate its radiological risks from samples of natural raw materials frequently used for both domestic and industrial purposes in Greece.

The following steps were taken to measure the activity:

a) Gamma-ray spectra of the prepared samples were measured using the low-background coaxial p-type HPGe detector. In order to obtain a good statistical accuracy, a sufficiently high counting measurement time (over 80000 pulses per second - ips) was used.

b) The energy peaks characteristic of gamma radiation corresponding to Ra 226, Th 232 U 238 and K 40 were identified in the measured spectra by comparing the energies of the detected peaks with the known energies of gamma rays from the disintegration of these radionuclides.

c) calibration of the detector efficiency was performed for the specific energies of the identified gamma-ray peaks. This calibration takes into account sample geometry, distance from the detector, and other factors that affect detection efficiency.

d) The detection efficiency for each gamma-ray energy was calculated using MAESTRO-32 software taking into account sample matrix, geometry and other corrections.

e) Calculation of the activity concentrations of Ra 226, Th 232 U 238 and K 40 in collected samples using the net peak area of the respective gamma ray peaks, the mass of the sample and the standard and the standard activity concentration for the selected radionuclides.

Equation 5.1 was used to calculate the activity concentrations of radionuclides (radium, thorium, potassium and uranium) from the samples prepared for analysis, table 5.1. Calculation of radioactive elements in the sample was done using Excel 2019.

$$C_p = \frac{I_p}{I_e} \times \frac{M_e}{M_p} \times C_e \quad 5.1$$

where:

C_p = concentration of radionuclide activity in the samples (Ra 226, Th 232 U 238 and K 40),

I_p = background-corrected sample photopic intensity (ips),

I_e = background-corrected photopic intensity of the standard (ips),

M_e = mass of the standard;

M_p = sample mass;

C_e = concentration of radionuclide activity in the standard (Ra 226, Th 232 U 238 and K 40).

The details of the calculation of the activities are given in the Calculation Sheets in ANNEX 1.

The final results of the calculations of the activity concentrations of the studied radionuclides (according to the calculation sheets) are centralized in Table 5.3 as follows: column 1, - the unique identification code of the sample; columns 2, 3, 4 and 5 the concentrations of the activities of the studied radionuclides K 40, Ra 226, 234Th and U 238, expressed in (Bq/kg).

Table 5.3. Concentrations of the activities of radionuclides U 238, Ra 226, Th 232 and K 40 in the studied samples in Bq/kg..

Cod.	K 40	Ra 226	Th 232	U 238
	(Bq/kg)			
G1	24,4	28,5	2,4	16,5
G2	8,1	2,9	1,0	1,0
G3	2,3	4,1	1,0	1,0
G4	10,2	14,2	1,1	10,8
G5	8,0	2,9	1,0	2,8
G6	8,0	14,3	1,0	7,7
G7	27,5	5,2	2,7	1,7
G8	8,0	3,9	1,0	3,5
G9	27,9	1,0	2,1	1,0
G10	4,0	0,7	1,0	2,1
G11	7,0	3,8	1,0	2,6
G12	8,0	4,6	1,0	6,3
G13	181,0	1,0	1,0	3,1
G14	548,0	38,2	48,3	30,8
G15	460,0	18,6	26,8	12,5
G16	65,8	14,7	14,9	12,9
G17	245,0	140,6	20,6	29,4
G18	356,0	184,5	24,3	74,2
Tabela 5.4 Prelucrarea statistică a datelor				
AVERAGE	111,07	26,89	9,01	12,21
STDEV:P	169,37	49,52	12,86	17,47
AVEDEV	137,18	31,58	10,21	11,45
GEOMEAN	27,93	8,04	3,23	5,55
Min	2,3	1	1	1
Max	548	184,5	48,3	74,2
alpha	0,05	0,05	0,05	0,05
Conf.T	68,22	15,71	5,08	5,69
Inter. Val.	111,07±68,22	26,88±15,71	8,94±5,08	12,7±5,69
Masa etalonului, $M_e = 62$ g				
Limita de detecție: K 40 = 8 Bq.kg ⁻¹ ; Ra 226 = U 238 = 234Th = 1 Bq.-kg ⁻¹				

Table 5.4 presents the concentrations of radionuclide activities, U 238, Th 232, Ra 226 and K 40 in (Bq/kg) determined following the primary data processing after reading the tracks on the CR39 detectors, for each of the measured samples. For the statistical processing of the data, from table 5.4, it was done by replacing the detection limits (LD) with their numerical values. The main results obtained are:

- U 238 AM is 12.21 (Bq/kg); confidence interval = 5.69 (Bq/kg), for $\alpha = 0.05$; The mean value of the activity concentration = 12.7 ± 5.69 (Bq/kg),
- Th 232, AM is 9.01 (Bq/kg); confidence interval = 5.08 (Bq/kg), for $\alpha = 0.05$; The mean value of the activity concentration = 8.94 ± 5.08 (Bq/kg),
- Ra 226, AM is 26.89 (Bq/kg); confidence interval = 15.71 (Bq/kg), for $\alpha = 0.05$; The mean value of the activity concentration = 26.88 ± 15.71 (Bq/kg),
- K 40, AM is 111.07 (Bq/kg); confidence interval = 111.07 (Bq/kg), for $\alpha = 0.05$; The mean value of the activity concentration = 111.07 ± 68.22 (Bq/kg),

5.2 Radiological parameters for the studied materials

For the calculation of the following radiological hazard indices: Equivalent radium activity (R_{aeq}), Total absorbed dose (DTA_{in}), Total effective annual dose equivalent in open air (D_{γ}), Annual external effective dose equivalent ($EDTA_{ex}$), Annual equivalent of internal effective dose ($EDTA_{in}$), External (H_{ex}) and internal (H_{in}) hazard indices, Gamma radiation activity index, I_{γ} , Alpha radiation index, I_{α} , Annual gonadal dose equivalent (AGDE), Excess cancer risk for lifetime (RCE) and Dose Criterion, equations 5.2 (§ 5.4.1), 5.3 – 5.13, (§ 5.5) were used and the results are presented in table 5.9.

Tabela 5.9. Prelucrarea statistică a concentrațiilor activității radionuclizilor K 40, Ra 226, Th 232 și U 238 și estimarea indicilor de pericol radiologic ai acestora pentru cele 18 probe studiate.

Cod.	Materialul de construcții	⁴⁰ K	²²⁶ Ra	²³² Th	²³⁸ U	I _γ	D _γ	DTA _{in}	Hex	H _{in}	Raeq	EDTA _{ex}	EDTA _{in}	I _a	AGDE	RCE	D _{criteria}	
		[Bq/kg]					[nGy/h]	[mSv/y]		[Bq/kg]	[mSv/y]	[mSv/y]						
G1	Mortar	24,4	28,5	2,4	16,5	0,115	15,63	30,81	0,091	0,168	33,81	0,019	0,077	0,143	105,76	0,0078	0,0457	
G2	Marmură culoare deschisă	8,1	2,9	1,0	1,0	0,017	2,28	4,42	0,013	0,021	4,95	0,003	0,011	0,015	15,68	0,0011	0,0067	
G3	Marmură Gri	2,3	4,1	1,0	1,0	0,019	2,59	5,06	0,015	0,027	5,71	0,003	0,013	0,021	17,57	0,0013	0,0077	
G4	Nisip	10,2	14,2	1,1	10,8	0,056	7,65	15,09	0,045	0,083	16,56	0,009	0,038	0,071	51,68	0,0038	0,0224	
G5	Marmură culoare deschisă	8,0	2,9	1,0	2,8	0,017	2,28	4,41	0,013	0,021	4,95	0,003	0,011	0,015	15,65	0,0011	0,0067	
G6	Marmură întunecată	8,0	14,3	1,0	7,7	0,055	7,54	14,90	0,044	0,083	16,35	0,009	0,037	0,072	50,88	0,0038	0,0221	
G7	Piatră naturală	27,5	5,2	2,7	1,7	0,040	5,18	9,95	0,030	0,044	11,18	0,006	0,025	0,026	35,99	0,0026	0,0151	
G8	Piatră naturală	8,0	3,9	1,0	3,5	0,021	2,74	5,33	0,016	0,027	5,95	0,003	0,013	0,020	18,74	0,0014	0,0080	
G9	Piatră naturală	27,9	1,0	2,1	1,0	0,023	2,89	5,46	0,017	0,019	6,15	0,004	0,014	0,005	20,63	0,0014	0,0083	
G10	Marmură albă	4,0	0,7	1,0	2,1	0,009	1,09	2,06	0,007	0,008	2,44	0,001	0,005	0,004	7,60	0,0005	0,0033	
G11	Marmură culoare închisă	7,0	3,8	1,0	2,6	0,020	2,65	5,16	0,016	0,026	5,77	0,003	0,013	0,019	18,12	0,0013	0,0078	
G12	Marmură culoare deschisă	8,0	4,6	1,0	6,3	0,023	3,06	5,97	0,018	0,030	6,65	0,004	0,015	0,023	20,91	0,0015	0,0090	
G13	Marmură galben închis	181,0	1,0	1,0	3,1	0,069	8,61	16,50	0,044	0,047	16,37	0,011	0,042	0,005	64,10	0,0043	0,0221	
G14	Cărămidă	548,0	38,2	48,3	30,8	0,552	69,67	132,11	0,404	0,507	149,47	0,085	0,342	0,191	492,00	0,0346	0,2015	
G15	Cărămidă	460,0	18,6	26,8	12,5	0,349	43,96	83,39	0,249	0,300	92,34	0,054	0,216	0,093	313,94	0,0219	0,1245	
G16	Ciment alb "Hercules"	65,8	14,7	14,9	12,9	0,145	18,53	35,18	0,111	0,151	41,07	0,023	0,091	0,074	128,37	0,0092	0,0554	
G17	Ciment negru "Hercules"	245,0	140,6	20,6	29,4	0,653	87,62	171,61	0,510	0,890	188,92	0,107	0,430	0,703	597,49	0,0436	0,2551	
G18	Ciment negru "Chalips"	356,0	184,5	24,3	74,2	0,855	114,76	224,95	0,666	1,165	246,66	0,141	0,563	0,923	783,46	0,0571	0,3331	
Valori recomandate de UNSCEAR 2000							59,00	84,00				0,700	0,410			0,0500		
Minim		2,3	0,7	1,0	1,0	0,008	1,09	2,06	0,007	0,008	2,44	0,001	0,005		7,60	0,0005		
Maxim		548,0	184,5	48,3	74,2	1,039	114,76	224,95	0,67	1,17	246,66	0,141	0,563		783,46	0,0571		
Media		111,1	26,9	8,5	12,2	0,169	22,15	42,91	0,13	0,20	47,52	0,027	0,109		153,25	0,0110		
STDEV.P		39,9	11,7	3,1	4,1	0,068	7,8	15,2	0,045	0,075	16,7	0,010	0,038		53,6	0,0039	0,0226	
AVEDEV		137,2	31,6	10,3	11,4	0,202	25,3	48,9	0,146	0,229	54,148	0,031	0,124		174,876	0,0126	0,0731	
GEOMEAN		27,9	7,9	2,8	5,6	0,050	8,1	15,6	0,047	0,071	17,4	0,010	0,040		55,9	0,0040		
Valoarile medii		137,2±39,9		10,3±3,1			25,3±7,4		48,9±15,2		0,229±0,075		0,031±0,01		174,87±53,6		0,073±0,023	
		31,6±11,7		11,4±11,4			0,146±0,045		54,148±16,7		0,124±0,038		0,126±0,039					

5.3 Conclusions.

The specific activity of the natural radionuclides U 238 (Ra 226), Th 232 and K 40 in samples of common building materials were found to be within the global average limits. Radium equivalent activity, external hazard index (Hex), internal hazard index (Hin), absorbed dose rate (D), annual effective dose equivalent (AEDE), gamma index (Ig) and annual gonadal dose equivalent (AGDE) were calculated and found to be within common values, with no significant radiation hazards arising from the use of such materials for building construction.

Human radiation exposure can be greatly increased due to the use of building materials containing high levels of naturally occurring radionuclides. Materials that are normally used in the construction industry, i.e. red clay bricks, cement, concrete, gravel and sand contain regulated levels of primary terrestrial radionuclides (K 40, Ra 226 and Th 232) and the absorbed dose rate in air for interior. does not exceed the dose criterion value of 80 nGy.h⁻¹ or 0.3 mSv.y⁻¹ for the individual effective dose (Giagias E., et.al.,2017).

The radioactivity content of the building materials is between: 2.3 and 548.0 Bq.kg⁻¹ for K 40; 0.7 and 184.5 Bq.kg⁻¹ for Ra 226; 1.0 and 48.3 Bq.kg⁻¹ for Th 232 and between 1.0 and 74.2 Bq.kg⁻¹ for U 238. The highest values were obtained for bricks and cements.

The absorbed dose of the studied construction materials has values $D_a < 80 \text{ nGy}\cdot\text{h}^{-1}$, except for black cement, where $D_a > 80 \text{ nGy}\cdot\text{h}^{-1}$.

The activity indices of the construction materials have low values ($I < 0.5$) in all collected samples, and only in brick and black cement have $I > 0.5$. The annual effective dose also have low values ($HE < 0.3$), except for brick. and black cement, where $HE > 0.3$ (Cosma .et.al., 2012; Pastepanou C, et.al., 2005)

6 SELECTIVE BIBLIOGRAPHY

Adelikhah M, Shahrokhi A, Chalupnik S, Tóth-Bodrogi E, Kovács T (2020) High level of natural ionizing radiation at a thermal bath in Dehloran, Iran. *Heliyon* 6:e04297.

Adhab Hiba Ghemeedh, Shaymaa Awad Kadhim alshebly, Dr. Emad Kareem Alsabari. **Assessment excess lifetime cancer risk of soils samples in Maysan neighborhood adjacent to the middle Euphrates cancer center in Najaf / Iraq.** 2020 IOP Conf. Ser.: Mater. Sci. Eng. 928 (2020) 072100, doi:10.1088/1757-899X/928/7/072100.

Adyasari et.al., 2023, Radon-222 as a groundwater discharge tracer to surface waters, *Earth Sci. Rev.*, № 238.

Ali, M. Y., Hanfiah, M. M., & Khan, M. F. (2018). Potential factors that impact the radon level and the prediction of ambient dose equivalent rates of indoor microenvironments. *Science of the Total Environment*, 626, 1–10. <https://doi.org/10.1016/j.scitotenv.2018.01.080>

- Al-Khateeb, H. M., Nuseirat, M., Aljarrah, K., Ali, M., Al-Akhras, H., & Bani-Salameh, H. (2017). Seasonal variation of indoor radon concentration in a desert climate. *Applied Radiation and Isotopes*, *130*, 49–53. <https://doi.org/10.1016/j.apradiso.2017.08.017>.
- Annunziata F. Michael; Radioactivity: Introduction and History, From the Quantum to Quarks, 2016, New; Hardcover. Condition: New/New; ISBN 10: 0444634894 Elsevier).
- Baeza, A., García-Paniagua, J., Guillén, J., & Montalbán, B. (2018). Influence of architectural style on indoor radon concentration in a radon prone area: A case study. *Science of the Total Environment*, *610-611*, 258–266. <https://doi.org/10.1016/j.scitotenv.2017.08.056>
- Baias P.F., W. Hofmann, R. Winkler-Heil, C. Cosma, O.G. Dului, *Radiation Protection Dosimetry* **138** (2), 111-118 (2009).
- Begy R., C. F. Savin, D. K. Süle, M. Nuhanovic, *Evanghelos Giagias*, T. Kovács, 2022, Radiological Investigation of Natural Carbonated Spring Waters from Eastern Carpathians, *Journal of Radioanalytical and Nuclear Chemistry*, *331*, 1439-1450 (2022).<https://doi.org/10.1007/s10967-022-08195-3>.
- Begy, IR. Cs. Sz. Kelemen, C. Savin, **Giagias Evangelos**, D. Ristoiu, 2020. Post-volcanic activities reflected in radionuclide content of spring waters from Romania, VII. Terrestrial Radioisotopes In Environment, International Conference on Environmental Protection, Ed. Edited by: Tibor Kovács, ISBN 978-615-81632-0-0, DOI 10.18428/TREICEP-2020.
- Behnam Zehtab, Khaleel. I. Noor, Hayder. H. Moula; Review on Concepts of Zero Energy Building, Design Engineering issue 9, 12354-12366, February 2022.
- Bena Eleonora, 2024, Giancarlo Ciotoli, Eric Petermann, Peter Bossew, Livio Ruggiero, Luca Verdi, Paul Huber, Federico Mori, Claudio Mazzoli, Raffaele Sassi, A new perspective in radon risk assessment: Mapping the geological hazard as a first step to define the collective radon risk exposure, *Science of the Total Environment* *912* (2024) 169569, <https://doi.org/10.1016/j.scitotenv.2023.169569>.
- Bena, E., Ciotoli, G., Ruggiero, L., Coletti, C., Bossew, P., Massironi, M., Mazzoli, C., Mair, V., Morelli, C., Galgaro, A., Morozzi, P., Tositti, L., Sassi, R., 2022. Evaluation of tectonically enhanced radon in fault zones by quantification of the radon activity index. *Sci. Rep.* *12*, 21586 <https://doi.org/10.1038/s41598-022-26124-y> .
- Boronkay, K., Stoumpos, G., Benissi, M., Rovolis, G., Korkkaris, K., Papastamatiou, D., Dimitriou, G., Chrysikopoulou, A., Miliotis, I., Giakoumis, A., Novack, M., & Marinou, P. (2021). Geological map of Athens Metropolitan Area, Attica (Greece): A review based on Athens Metro ground investigation data. *Bulletin of the Geological Society of Greece*, *57*(1), 68–126. <https://doi.org/10.12681/bgsg.26895>.
- Bossew P., Cinelli G., Tollefsen T., De Cort M., 2017. The Geogenic Radon Hazard Index – Another Attempt. *IWEANR (Intl. Workshop on the European Atlas of Natural Radiation)*. November 2017. <https://remon.jrc.ec.europa.eu/About/Atlas-of-Natural-Radiation/Geogenic-radon/Geogenicradon> (accessed June 6, 2018).
- Bossew, P., 2015. Mapping the Geogenic Radon Potential and Estimation of Radon Prone Areas in Germany. *Radiation Emergency Medicine* *4* (2), 13–20.
- Bossew, P., Cinelli, G., Ciotoli, C., Crowley, Q.G., De Cort, M., Medina, J.E., Gruber, V., Petermann, E., Tollefsen, T., 2020. Development of a geogenic radon hazard index – concept, history, experiences. *Int. J. Environ. Res. Public Health* *17* (11), 4134. <https://doi.org/10.3390/ijerph17114134>.
- Bossew, P., Cinelli, G., Ciotoli, G., Crowley, Q. G., De Cort, M., Medina, J. E., Gruber, V., Petermann, E., & Tollefsen, T. (2020). Development of a geogenic radon hazard index - concept, history, experiences. *International Journal of Environmental Research and Public Health*, *17*(11), 1–23. <https://doi.org/10.3390/ijerph17114134> .
- Bouder, F.; Perko, T.; Lofstedt, R.; Renn, O.; Rossmann, C.; Hevey, D.; Siegrist, M.; Ringer, W.; Pözl-Viol, C.; Dowdall, A.; et al. (2021) The Potsdam radon communication manifesto. *J. Risk Res.* **2021**, *24*, 909–912.
- Building materials, accessed 28.09.2023, <https://nucleus.iaea.org/sites/orpnet/training/norm/Shared%20Documents/Building%20Materials.pdf>.
- Burghel et al., 2019, The first large-scale mapping of radon concentration in soil gas and water in Romania, *Sci. Total Environ.*, № 669, c. 887 <https://doi.org/10.1016/j.scitotenv.2019.02.342>.
- Calculating GSD, 2023, <https://www.mrexcel.com/board/threads/calculating-geometric-standard-deviation-with-range-including-blanks.1211206/> , accessed 23.09.2023

- Cinelli, G., Brattich, E., Coletti, C., De Ingeniis, V., Mazzoli, C., Mostacci, D., ... Tositti, L. (2020). Terrestrial gamma dose rate mapping (Eugane Hills, Italy): comparison between field measurements and HPGe gamma spectrometric data. *Efecte ale radiațiilor și defecte în solide*, 175 (1–2), 54–67. <https://doi.org/10.1080/10420150.2020.1718131>.
- Cinelli, G.; Tollefsen, T.; Bossew, P.; Gruber, V.; Bogucarskis, K.; De Felice, L.; De Cort, M. Digital Version of the European Atlas of Natural Radiation. *J. Environ. Radioact.* **2018**. doi:10.1016/j.jenvrad.2018.02.008.
- Ciotoli G, Voltaggio M, Tuccimei P, Soligo M, Pasculli A, Beaubien SE, Bigi S (2017) Geographically weighted regression and geostatistical techniques to construct the geogenic radon potential map of the Lazio region: A methodological proposal for the European Atlas of Natural Radiation. *J. Environ. Radioact.* 166, 355–375.
- Coleman, M.J., Schneider, D.A., Grasemann, B., Soukis, K., Lozios, S., Hollinetz, M.S., 2020. Lateral Termination of a Cycladic-Style Detachment System (Hymittos, Greece). *Tectonics*, 39, 1–30. <https://doi.org/10.1029/2020TC006128>.
- Commission Recommendation (EU). 2019/786 of 8 May 2019 on building renovation, C/2019/3352. Official Journal of the European Union. L127/34. Retrieved October 15, 2020, from Europa.eu website: <https://eur-lex.europa.eu/legal-content/EN/TXT/PDF/?uri=CELEX:32019H0786&from=GA> (2019).
- Cosma C, Ristoiu D, Poffijn A, Meesen G. Radon in various environmental samples in the Herculane spa, Cerna valley, Romania. *Environ Int* (1996) **22**(Suppl 1):S383–8. doi:10.1016/S0160-4120(96)00136-5.
- Cosma C., A. Poffijn, D. Ristoiu, G. Meesen, Some Aspects of Radon Radioactivity in Herculane Spa (Romania), *Environment International*, 24, 1 - 4 (1996).
- Cosma C., Dicu T., Dinu A., Begy R. (2009b), Radon and lung cancer, Ed. Quantum, Cluj-Napoca, ISBN 978-973-88835-2-9, 166 pp.
- Cosma C., Szacsvai K., Dinu A., Ciorba D., Dicu T., Suci L., 2009a Preliminary integrated indoor radon measurements in Transilvania (Romania). *Isotopes in Environmental and Health Studies* 45(2):1–10.
- Cosma Constantin, Alexandra Cucuș (Dinu), Botond Papp, Robert Begy, Alida Gabor, Nicoleta Bican-Brișan & Lucian Beșuțiu, Radon Implication in Life and Earth Science: Băița-Ștei Area and Peceneaga-Camena Fault (Romania), *Carpathian Journal of Earth and Environmental Sciences*, May 2014, Vol. 9, No. 2, p. 15 - 21.
- Cosma Constantin, O. A. Dumitru, Dan Constantin Niță, Robert Begy, Alexandra Cucuș, Andra Iurian, Mircea Moldovan, Botond Papp, Tiberius Dicu, Betty Burghel, Liviu Suci, Carlos Sainz, **Evanghelos Giagias** 2012. Preliminary results of natural radioactivity measurements in some building materials from uranium mine area Băița, Romania by gamma spectrometry. *ECOTERRA - Journal of Environmental Research and Protection* 2012, Vol. 12, Nr.33.
- Cosma, C., Cucuș (Dinu), A., Dicu, T., 2012. Spre prima hartă a concentrației rezidențiale de radon din România. *Radioprotecție Dozimetrie*.
- Cosma, C., Cucuș, A., Papp, B., Begy, R., Dicu, T., Moldovan, M., et al. (2013). Radon measurements and radon remediation in Băița-Ștei prone area. *Carpathian Journal of Earth and Environmental Sciences*, 8(2), 191–199.
- Cosma, C., Cucuș-Dinu, A., Papp, B., Begy, R., Sainz, C., *Soil and building material as main sources of indoor radon in Băița-Ștei radon prone area* (Romania), 2013, *Journal of Environmental Radioactivity*, 2013, 116, 174-179. DOI: 10.1016/j.jenvrad.2012.09.006.
- Cosma, C., Dicu, T., Dinu, A., Begy, R. (Eds.), *Radon and lung cancer*, Editura Quantum, Cluj-Napoca, ISBN 978-973-88835-2-9, 166 pp, 2009.
- Cucuș (Dinu) A., Cosma C., Dicu T., Begy R., Moldovan M., Papp B., Niță D., Burghel B., Sainz C., 2012 Thorough investigations on indoor radon in Băița radon-prone area (Romania). *Science of the Total Environment* 431(1):78-83.
- Cucos (Dinu) A., S. Vasiliniuc, A. Timar-Gabor, P. Manea, C. Cosma, 2014, *Contribution of radon dose to the patient exposure in the mofette of Covasna sanatorium, Romania, August 2014* [Carpathian Journal of Earth and Environmental Sciences](https://doi.org/10.1016/j.jenvrad.2012.09.006) Vol. 9, No. 3(3):69-74.
- Cucuș (Dinu), A., Dicu, T. & Cosma, C. 2015b, Indoor radon exposure in energy-efficient houses from Romania. *Rom. J. Phys.* **60**, 1574–1580 (2015).
- Cucuș (Dinu), **E. Giagias**, C. Cosma, 2015a, Indoor radon exposure in energy-efficient houses from Romania,

ENVIRA 2015, THESSALONIKI GREECE, 21-25 Septembrie 2015.

Deligiannakis, G., Papanikolaou, I.D., Roberts, G., 2018. Fault specific GIS based seismic hazard maps for the Attica region, Greece. *Geomorphology*, 306, 264–282. <https://doi.org/10.1016/j.geomorph.2016.12.005>.

Dicu T., B. D. Burghel, M. Botoș, A. Cucos, G. Dobrei, Ș. Florică, Ș. Grecu, A. Lupulescu, I. Papl, K. Szacsvai, A. Țenter & C. Sainz, 2021, A new approach to radon temporal correction factor based on active environmental monitoring devices, *Scientific Reports* | (2021) 11:9925, www.nature.com/scientificreports <https://doi.org/10.1038/s41598-021-88904-2>.

Dinu Alexandra, Dicu T., Cosma C., Biological effects of ionising radiations- Radioprotection, Environment & Progress 6/2006, 13-15 octombrie 2005 Agnita, Vol. 6/2006, p. 149-156, 2006.

Directiva 2010/31/UE a Parlamentului European și a Consiliului, 19.05.2010, privind performanța energetică a clădirilor.

Directive (EU) 2018/844 on the energy performance of buildings of the European Parliament and of the Council of 30 May 2018.

Dorrah, DH, Marzouk, M.: Integrated multi-objective optimization and agent-based building occupancy modeling for space planning. *Journal of Building Engineering* 34, 101902 (2021). <https://doi.org/10.1016/j.job.2020.101902>.

Du, L. *et al.* Effects of energy retrofits on Indoor Air Quality in multifamily buildings. *Indoor Air* **29**, 686–697 (2019).

Florică, Ș., Burghelo, B.-D., Bican-Brișan, N., Begy, R., Codrea, V., Cucos, A., Catalina, T., Dicu, T., Dobrei, G., Istrate, A., Lupulescu, A., Moldovan, M., Niță, D., Papp, B., Papp, I., Szacsvai, K., Țenter, A., Sferle, T., & Sainz, C. (2020). The path from geology to indoor radon. *Environmental Geochemistry and Health*, 42(9), 2655–2665. <https://doi.org/10.1007/s10653-019-00496-z>.

Ganas, A.; Tsironi, V.; Kollia, E.; Delagas, M.; Tsimi, C.; Oikonomou, A. 2018, Recent upgrades of the NOA database of active faults in Greece (NOAFAULTs). In Proceedings of the 19th General Assembly of WEGENER, Grenoble, France, 10–13 September 2018.

Georgiou E. K. Natalles, M. Molfetas, A. Athanassiadis, C Proukakis 1986, Radon measurement in Greece, *Nucl. Med.* 25, A136.

Geysmans, R.; Perko, T.; Keser, M.; Pözl-Viol, C.; Fojtková, I.; Mihók, P. Cure or Carcinogen? A Framing Analysis of European Radon Spa Websites. *Int. J. Public Health* **2022**, 67, 1604559.

Giagias E. C. Cosma, D. Marcu, 2015a, Radon indoor concentration and its seasonal variation in Athens, Greece, ENVIRA 2015, Thessaloniki Greece.

Giagias E., D. Burghel, C. Cosma, (2015b), Seasonal Variation Of Indoor Radon In Dwellings From Athens, Greece, *Rom. Journ. Phys.*, Vol. 60, Nos. 9–10, P. 1581–1588, Bucharest, 2015.

Giagias E., Papp B., Ristoiu D., Cosma C., Simpozionul național cu participare internațională Environment & Progress 2017, 15 noiembrie 2017, Cluj-Napoca, România.

Giagias Evangelos, Botond PAPP, Dumitru RISTOIU, Constantin COSMA, (2017). Radioactivity of building materials from Greece, *Lucrare în Procceding, SIMPOZIONUL NATIONAL CU PARTICIPARE INTERNAȚIONALĂ ENVIRONMENT & PROGRESS 10 NOIEMBRIE 2017, CLUJ-NAPOCA, ROMANIA.*

Giagias Evangelos, 2013, New two-storey house with basement, ground floor garage & pool, Energy Rating: A+, project New Epidavros, 113 Themistokleous Str. 184 52 Nice, Athens GB_white, 2013.

Giagias Evangelos, Botond PAPP, Dumitru RISTOIU, Constantin COSMA, 2017. Radioactivity of construction materials commonly used in Greece, Poster, *SIMPOZIONUL NATIONAL CU PARTICIPARE INTERNAȚIONALĂ ENVIRONMENT & PROGRESS 10 NOIEMBRIE 2017, CLUJ-NAPOCA, ROMANIA.*

Giagias Evangelos, D. Burghel, C. Cosma, 2015, Seasonal variation of indoor radon in dwellings from Athens, Greece, *Rom. Journ. Phys.*, Vol. 60, Nos. 9–10, P. 1581–1588, Bucharest, 2015.

Giagias Evangelos, C. Cosma and D. Marcu, 2015, Radon Indoor Concentration and its Seasonal Variation in Athens, Greece, *In Conference proceedings. International Conference on environmental Radioactivity (ENVIRA) 2015* (pp. 205).

Giraldo-Osorio et.al., 2021, Residential radon in Manizales, Colombia: results of a pilot study, *Int. J. Environ. Res. Public Health*, № 18, c. 1228 <https://doi.org/10.3390/ijerph18031228>.

- Gruber, V., Baumann, S., Wurm, G., Ringer, W., & Alber, O. (2021). The new Austrian indoor radon survey (ÖNRAP 2, 2013–2019): Design, implementation, results. *Journal of Environmental Radioactivity*, 233(106618), 106618–106619. <https://doi.org/10.1016/j.jenvrad.2021.106618>IAEA.
- Hazou Eyakifama, Tchilabalo E. Patchali, Assessment of radiological hazards in the phosphate mining area of Kpogamé, Togo, *Case Studies in Chemical and Environmental Engineering*, Volume 3, June 2021, 100077.
- ICRP, (2018), Summary of ICRP Recommendations on Radon; 2018.
- IEA 2017, Insights Series 2017, Renewable Energy for Industry From green energy to green materials and fuels, Ed. Philbert Cedric, www.iea.org .
- IEA. World Energy Outlook 2021 <https://www.iea.org/reports/world-energy-outlook-2021> (International Energy Agency, 2021).
- Ioannides K., D. Patiris and C. Papachristodoulou, Indoor radon concentrations in workplaces and dwellings in North-Western Greece, *Radioprotection* 44, 165-169 (2009).
- IPCC AR6,2023: Summary for Policymakers. In: Climate Change 2023: Synthesis Report. Contribution of Working Groups I, II and III to the Sixth Assessment Report of the Intergovernmental Panel on Climate Change (Core Writing Team, H. Lee and J. Romero (eds.)). IPCC, Geneva, Switzerland, pp. 1-34, doi: 10.59327/IPCC/AR6-9789291691647.001.
- Khan I.U., Z. Qin, T. Xie, Z. Bin, H. Li, W. Sun, E. Lewis. Evaluation of health hazards from radionuclides in soil and rocks of North Waziristan, Pakistan. *International Journal of Radiation Research*, April 2020, Volume 18, No 2, 243-253.
- Kinga Hening 2015. Utilizarea detectorilor de urme în studiul Radonului: Expunere rezidențială și instituțională, Teză de doctorat, Universitatea „BABEȘ-BOLYAI” Cluj-Napoca Facultatea de Știința Mediului, 2015.
- Kolovou Maria, Constantinos Potiriadis, Nikolaos Kallithrakas-Kontos, A study on the correlation between indoor radon concentrations and the construction year of the dwellings, *The European Physical Journal Special Topics*. May 2023, Eur. Phys. J. Spec. Top. (2023) 232:1625–1629, <https://doi.org/10.1140/epjs/s11734-023-00888-4>.
- Kritidis P., V. Kamenopoulou, N. Kallithrakas-Kontos, Indoor radon concentrations in Athens determined with an optimized etched track detector technique, *Radiation Protection Dosimetry*, Volume 55, Number 2, September 1, 1994, pages 149–152.
- Kumar et.al., 2022, Radon exhalation potential and natural radioactivity in soil collected from the surrounding area of a thermal power plant, *J. Radioanal. Nucl. Chem.*, № 331, c. 2597.
- Lewis, S. L. & Maslin, M. A. (2015) Defining the Anthropocene, *Nature*, 519, 171-180.
- Marinos, G., Katsikatsos, G., Mirkou - Peripopoulou, R.M., 1974. The Athens' Schists Formation, II. Stratigraphy and Structure. *Annales Géologiques des Pays Helléniques*, 25, 439–444 (in Greek).
- Meyer M., Impact of constructional energy-saving measures on radon levels indoors, *Indoor Air* 29 (4) (2019) 680–685.
- NetZero Energy Commercial Building Initiative. (2017). U.S. Department of Energy. Retrieved from https://www1.eere.energy.gov/buildings/publications/pdfs/alliances/cbi_fs.pdf .
- Nezmal, M., Nezmal, M., Malotín, M., Barnet, I., Mikšová, J., *The new method for assessing the radon risk of building sites*, Special Papers No.16. Czech Geol. Survey. Praha, 2004.
- Ngarambe, J.; Oh, J.W.; Su, M.A.; Santamouris, M.; Yun, G.Y. Influences of wind speed, sky conditions, land use and land cover characteristics on the magnitude of the urban heat island in Seoul: An exploratory analysis. *Sustain. Cities Soc.* 2021, 71, 102953.
- Nikolopoulos D. Anna Louizi ,Virginia Koukouloub, Athina Serefoglou ,Evangelos Georgiou, Konstantinos Ntalles, Charalambos Proukakis. 2002, Radon survey in Greece—risk assesment, *J. Environ. Radioactivity* 63 (2002) 173–186. PII: S02 65 -931X(02)00026-7 Elsevier Science Ltd, www.elsevier.com/locate/jenvrad.
- Nikolopoulos D., E. Vlamakis, N. Chatzisavvas, P. H.Yannakopoulos, X. Argyriou1, E. Petraki, S. Kottou, T. Sevvos, N. Temenos, Y. Chaldeos, S. Filtisakos, N. Gorgolis, S. Potozi, Koulogliotis, A. Zisos. 2013, Study of the response of open CR-39 detector to radon and progeny by Monte Carlo simulation with SRIM 2013. *International Scientific Conference eRA-8*, 2013 ISSN-1791-1133 1.

- Nikolopoulos, D., Maddison, S., Louizi, A., & Proukakis C, 1997. Radon survey in Kriti-Greece. Design, implementation and results. In Proceedings of the European Conference on Protection against radon at home and at work. Praha, 156–159.
- ORDINUL nr. 2.223, 13 10. 2023, REGLEMENTARE TEHNICĂ din 13 octombrie 2023, RTC 7 - 2022, Monitorul Oficial al României, Partea I, nr. 973/26.X. 2023.
- Ordinul nr.152, 27.07.2023, Metodologia pentru determinarea concentrației de radon în aerul din interiorul clădirilor și de la locurile de muncă, Monitorul Oficial al României, Partea I, Nr. 729/8.VIII.2023, 3-14.
- Pampuri, L., Caputo, P. & Valsangiacomo, C. Effects of buildings' refurbishment on indoor air quality. Results of a wide survey on radon concentrations before and after energy retrofit interventions. *Sustain. Cities Soc.* **42**, 100–106 (2018).
- Papaefthymiou H., Maurodis A., Kritidis P., 1999, Indoor radon measurements in Patras, Greece, with solid state nuclear track detectors, *Radon in the Living Environment*: 385-390.
- Papanikolaou, D., Lozios, S., Soukis, K., Skourtsos, Em., 2004. The geological structure of the allochthonous "Athens Schists". *Bulletin of the Geological Society of Greece*, 36, 1550–1559 (in Greek).
- Papanikolaou, D., Papanikolaou, I., 2007. Geological, geomorphological and tectonic structure of NE Attica and seismic hazard implications for the northern edge of the Athens plain. *Bulletin of the Geological Society of Greece*, 40, 425–438.
- Papanikolaou, D.; Bargathi, H.; Dabovski, C.; Dimitriu, R.; El-Hawat, A.; Ioane, D.; Kranis, H.; Obeidi, A.; Oaie, G.; Seghedi, A.; et al. (2015), TRANSMED Transect VII: East European Craton–Scythian-Platform–Dobrogea–Balkanides–Rhodope-Massif–Hellenides–East Mediterranean–Cyrenaica. 2015.
- Papanikolaou, I.D., Roberts, G., Deligiannakis G., Sakellariou, A. and Vassilakis E., 2013. The Sparta Fault, Southern Greece: From segmentation and tectonic geomorphology to seismic hazard mapping and time dependent probabilities, *Tectonophysics*, <http://dx.doi.org/10.1016/j.tecto.2012.08.031>.
- Papastefanou C., Stoulos S., Manolopoulou M., 2005, The radioactivity of building materials. *J. Radioanal.Nucl.Chem.*, 266 (3), p.367-372.
- Papazachos, B.C., Comninakis, P.E., Karakaisis, G.F., Karakostas, B.G., Papaioannou, C.A., Papazachos, C.B. and Scordilis, E.M., 2000. A catalogue of earthquakes in Greece and surrounding area for the period 550BC–1999, Publication of the Geophysical Laboratory, University of Thessaloniki.
- Papp, B., Cosma, C., Moldovan, M., Niță, D.C., (2009a), Radon potential in soil and radon risk estimation. *ECO TERRA*, 22-23, p.42-44, (ISSN 1584-7071).
- Papp, B., Cosma, C., Niță, D.C., Moldovan, M., (2009b), Soil Radon Measurements in Cluj-Napoca (Romania). *V. Magyar Radon Fórum, Pannon Egyetem Kiadó, Veszprém*, p.55-60, (ISBN: 978-963-9696-78-5).
- Papp, B.**, Szakacs, A., Neda, T., Papp, Sz., Cosma, C., (2010), *Soil radon and thoron studies near the mofettes at Harghita Bai (Romania) and their relation to the field location of fault zones*. *Geofluids*, **10** (4), p.586–593. (I.F: 1,268 / 2010).
- Papp, Botond ; Cosma, Constantin ; Cucos (Dinu), Alexandra ; Suci, Liviu ; Dumitru, Oana Alexandra ; Banciu, Gheorghe ; Sainz, Carlos, Implementation of radon remediation techniques in houses in the uranium area of Baita-Steii (Romania), International Symposium "Environment and Industry" SIMI 2013, Volume II. <http://hdl.handle.net/123456789/406>.
- Poffijn A., M. Tirmarche, L. Kreienbrock, P. Kayser, S. Darby, Radon și cancer pulmonar: protocol și proceduri ale studiilor multicentrice în regiunea Ardennes-Eifel, Bretania și regiunea masivului central, *Dozimetrie de protecție împotriva radiațiilor*, volumul 45, numărul 1-4, 1 decembrie 1992, paginile 651–656, <https://doi.org/10.1093/rpd/45.1-4.651>.
- Radon Map, Grecia. <https://eeae.gr/en/radon-map> (accesat 22.07.2023).
- Rafferty 2023, What's the Difference Between Global Warming and Climate Change? Rafferty John P., Ed. Encyclopaedia Britannica, <https://www.britannica.com/story/whats-the-difference-between-global-warming-and-climate-change>, accesat 20.09.2023.
- Ruddiman, W.F. (2001, 2008, 2014). *Earth's Climate: past and future*, Third edition, ISBN-13: 978-1-4292-5525-7, W.H. Freeman & Sons. New York, NY.3., www.whfreeman.com.

- Sahoo et.al., 2020, Identification of earthquake precursors in soil radon-222 data of Kutch, Gujarat, India using empirical mode decomposition-based Hilbert Huang Transform, *J. Environ. Radioact.*, № 222 <https://doi.org/10.1016/j.jenvrad.2020.106353>.
- Sainz C., Dinu A., Dicu T., Szacsvai K., Quindós L. S., Cosma C., 2009 Comparative risk assessment of residential radon exposures in two radon-prone areas, Stei (Romania) and Torrelodones (Spain). *Sci Total Environ* 407(15):4452-4460.
- Sameh H. Negm, Wael M. El Maadway, Amal S. Nasr. Geochemical behavior and radiological hazards assessment of phosphorites at the eastern part of the economic phosphate-belt, Egypt. *Journal of Research in Environmental and Earth Sciences* Volume 9 ~ Issue 2 (2023) pp: 01-17 ISSN(Online) :2348-2532.
- Savin Codrin - Savian, **Evangelos Giagias**, David Karoly Sule, Robert-Csaba Begy. A new approach for determination of gross α/β activity in water samples by integrating Liquid Scintillation Counting with beta spectroscopy. *International Conference on radiation in various field of research*, 140. June 13-17, 2022, Herceg Novi, Montenegro. <https://doi.org.rad.spr.abstract.book.2022.28.14>.
- Schellnhuber HJ, Rahmstorf S, Winkelmann R (2016) Why the right climate target was agreed in Paris. *Nat Clim Change* 6:649–653.
- Schmid, S.M., Fügenschuh, B., Kounov, A., Maţenco, L., Nievergelt, P., Oberhänsli, R., Pleuger, J., Schefer, S., Schuster, R., Tomljenović, B., Ustaszowski, K., van Hinsbergen, D.J.J., 2020. Tectonic units of the Alpine collision zone between Eastern Alps and Western Turkey. *Gondwana Research*, 78, 308–374. <https://doi.org/10.1016/j.gr.2019.07.005>.
- Scotese Christopher, Benjamin Mills, Douwe van der Meer, (2021) Phanerozoic Paleotemperatures: The Earth's Changing Climate during the Last 540 million years. *Earth-Science Reviews*, 215. 103503. ISSN 0012-8252.
- Shahrokhi A, Adelikhah M, Chalupnik S, Kocsis E, Toth-Bodrogi E, Kovács T (2020) Radioactivity of building materials in Mahallat Iran – an area exposed to a high level of natural background radiation – attenuation of external radiation doses. *Mater Constr* 70;-233.
- Shahrokhi A, Adelikhah M, Chalupnik S, Kovács T (2021) Multivariate statistical approach on distribution of natural and anthropogenic radionuclides and associated radiation indices along the north-western coastline of Aegean Sea Greece. *Mar Pollut Bull* 163:112009.
- Smit H.A.P. & J. Bezuidenhout, 30 Aug 2023), *Geology and climate: a novel method to estimate indoor radon exposure risk in South Africa*, *SOUTH AFRICAN GEOGRAPHICAL JOURNAL*, August 2023, <https://doi.org/10.1080/03736245.2023.2253197>, <https://www.tandfonline.com/loi/rsag20>.
- Smit, H. A. P., & Bezuidenhout, J. (2021). Influence of climate and weather on the mitigation of radon exposure in two towns of the Western Cape, South Africa. *Journal of Radiation Research & Applied Sciences*, 14(1), 236–245. <https://doi.org/10.1080/16878507.2021.1940750>.
- Smith, Peter F., *Architecture in a Climate of Change, A guide to sustainable design*, 295 pp., First published 2001, Second edition 2005, Architectural Press, An imprint of Elsevier.
- Steffen W, Broadgate W, Deutsch L, Gaffney O, Ludwig C (2015) The trajectory of the Anthropocene: The great acceleration. *Anthropocene Rev* 2:81–98.
- Steffen Will,b,1,(2018) Johan Rockströma, Katherine Richardsonc, Timothy M. Lentond, Carl Folkea,E., Diana Livermanf, Colin P. Summerhayesg, Anthony D. Barnoskyh, Sarah E. Cornellia, Michel Crucifixi,J., Jonathan F. Dongesa,K., Ingo Fetzer, Steven J. Ladea,B., Marten K.Schefferl, Ricarda Winkelmannk,M, and Hans Joachim Schellnhuber, K.L.M., *Trajectories of the Earth System in the Anthropocene*, Edited by William C. Clark, Harvard University, Cambridge, MA, and approved July 6, 2018 (received for review June 19, 2018., *Proceedings of the National Academy of Sciences -PNAS*, August 14, 2018, vol. 115, no. 33, 8252–8259; DOI:10.1073/pnas.1810141115. (This open access article is distributed under Creative Commons Attribution-NonCommercial-NoDerivatives License 4.0 (CC BY-NC-ND)., information online at www.pnas.org/lookup/suppl/doi:10.1073/pnas.1810141115/-/DCSupplemental . Published online August 6, 2018.
- Sukanya et.al., 2023, Application of radon (²²²Rn) as an environmental tracer in hydrogeological and geological investigations: an overview, *Chemosphere*, № 303, <https://doi.org/10.1016/j.chemosphere.2022.135141>.
- Truță-Popa L. A., Dinu A., Dicu T., Szacsvai K., Cosma C., Hofmann W., 2010 Preliminary lung cancer risk assessment of exposure to radon progeny for Transylvania, Romania. *Health Physics* 99(3):301-307.

- Tsodoulos, I.M., Koukouvelas, I.K., Pavlides, S., 2007. Tectonic geomorphology of the easternmost extension of the Gulf of Corinth (Beotia, Central Greece). *Tectonophysics*, 453, 211–232, doi: 10.1016/j.tecto.2007.06.015.
- Tzani A., A. Efstathiou, S. Chailas, E. Lagios, M. Stamatakis, 2020, The Methana Volcano – Geothermal Resource, Greece, and its relationship to regional tectonics, *Journal of Volcanology and Geothermal Research*, 404, (2020). <https://doi.org/10.1016/j.jvolgeores.2020.107035>.
- UNEP 2021, Emissions Gap Report 2021: The Heat is On – A World of Climate Promises Not Yet Delivered <https://www.unep.org/resources/emissions-gap-report-2021> (United Nations Environment Programme, 2021).
- UNSCEAR 2020/2021 REPORT VOLUME II: " Sources, Effects and Risk of Ionizing Radiation", Annex B: Levels and effects of radiation exposure due to the accident at the Fukushima Daiichi Nuclear Power Station: implications of information published since the UNSCEAR 2013 Report, 2022.
- UNSCEAR 2020/2021 REPORT VOLUME IV: " Sources, Effects and Risk of Ionizing Radiation", Annex D - Evaluation of occupational exposure to ionizing radiation, 2022.
- UYANIK N. Ayten 2022. An Alternative Approach to the Excess Lifetime Cancer Risk and Prediction of Radiological and Cancer Risks Caused by Terrestrial Radiation, Case of Isparta/Turkey. August 19th, 2022, <https://doi.org/10.21203/rs.3.rs-1929990/v1>.
- Vogiannis, 2004, E., Nikolopoulos, D., Louizi, A., Halvadakis, C.P, 2004. Radon variations during treatment in thermal spas of Lesbos Island (Greece). *J. Environ. Radioactiv.* 75, 159-170.
- Vogth (Tecşa) Viorica, Bety Burghel, Alexandra Cucos, Dorin Iancu, Constantin Cosma, Ionut T. Moraru, **Evanghelos Giagias**, 2015. Preliminary results regarding the risk of lung cancer caused by radon exposure in Alba Iulia and surroundings. *ECOTERRA- Journal of Environmental Research and Protection* 2015, Vol. 12, Nr.14 (pp. 13-18).
- WHO (World Health Organization). *WHO Handbook on Indoor Radon: A Public Health Perspective*. WHO ISBN 978 92 4 154767 3. 2009. http://www.who.int/ionizing_radiation/env/radon/en/index1.html (accessed June 6, 2018).
- World Life Expectance, (2020), <https://www.worldlifeexpectancy.com/ro/greece-life-expectancy> 2020) accesat 05.03. 2023.
- Xie, D., Wu, Y., Wang, C., Yu, C. W., Tian, L., & Wang, H. (2021). A study on the three-dimensional unsteady state of indoor radon diffusion under different ventilation conditions. *Sustainable Cities and Society*, 66, 102599. <https://doi.org/10.1016/j.scs.2020.102599>.
- Xue et.al., 2021, Bedrock radon concentration in the Qingdao urban planning area and its bearing on lithology, *Marine Geol. Front.*, № 37, c. 10.
- Zhang Shengrong, Doudou Jin, Huijun Jin, Chunhai Li, Hu Zhang, Xiaoyin Jin, Jian Cui, 2024, Potential radon risk in permafrost regions of the Northern Hemisphere under climate change: A review, [Earth-Science Reviews Volume 250](#), March 2024, 104684.
- Zhou et.al., 2017, Degassing of CO₂, CH₄, Rn and Hg in the rupture zones produced by Wenchuan M. 8.0 earthquake, *Acta Petrol. Sin.*, № 33, c. 291.
- Zhuo, 2021, Estimating the amount and distribution of radon flux density from the soil surface in China, *J. Environ. Radioact.*, № 99, c. 1143, <https://doi.org/10.1016/j.jenvrad.2008.01.011>